Soft Matter

Accepted Manuscript

ROYAL SOCIETY OF CHEMISTRY

www.rsc.org/softmatter

Recent Advances in Clay Mineral-Containing Nanocomposite Hydrogels

Li Zhi Zhao,[a] Chun Hui Zhou,[a,b,c]* Jing Wang,[c] Dong Shen Tong,[a]

Wei Hua Yu,[a] Hao Wang[c,]*

[a] *Research Group for Advanced Materials & Sustainable Catalysis (AMSC), State Key Laboratory Breeding Base of Green Chemistry-Synthesis Technology, College of Chemical Engineering, Zhejiang University of Technology, Hangzhou 310032, China*

[b] *Key Laboratory of Clay Minerals of Ministry of Land and Resources of The People's Republic of China, Engineering Research Center of non-metallic minerals of Zhejiang Province, Zhejiang Institute of Geology and Mineral Resource, Hangzhou 310007, China*

[c] *Centre of Excellence in Engineered Fibre Composites, University of Southern Queensland, Toowoomba, Queensland 4350, Australia*

Correspondence to: Prof. C H Zhou E-mail: clay@zjut.edu.cn; Chun.Zhou@usq.edu.au

ABSTRACT

Clay mineral-containing nanocomposite hydrogels have proven to be exceptional in composition, properties, and applications, and a significant amount of research has been performed over the past few years. The objective of this paper is to summarize and evaluate scientific advances in clay mineral-containing nanocomposite hydrogels and their specific preparation, formation mechanism, properties, and applications, and to identify the prevailing challenges and future directions of the field. The state-of-the-art of existing technologies and insights into the exfoliation of layered clay minerals, in particular montmorillonite and laponite, are discussed first. The formation and structural

characteristics of polymer/clay nanocomposite hydrogels made from *in situ* free radical polymerization, supramolecular assembly, and freezing–thawing cycles are then examined. Studies indicate that additional hydrogen bonding, electrostatic interactions, coordination bonds, hydrophobic interaction and even covalent bonds could occur between the clay mineral nanoplatelets and polymer chains, thereby leading to the formation of a unique three-dimension network. Accordingly, the hydrogels exhibit exceptional optical, mechanical properties, swelling-deswelling behavior, and stimuli-responsiveness, reflecting the remarkable effects of clay minerals. With the pivotal roles of clay minerals in the clay mineral-containing nanocomposite hydrogels, the nanocomposite hydrogels possess great potential as superabsorbents, drug vehicles, tissue scaffolds, wound dressing, and biosensors. Future work shall lay emphasis on the future studies on formation mechanisms with in-depth insights into interfacial interactions, tactical functionalization of clay minerals and polymers for desired properties, and expanding the applications.

Keywords: Clay minerals; Nanoplatelets; Polymers; Nanocomposite hydrogels; Superabsorbents; Biomaterials

1. Introduction

Hydrogels commonly refer to a class of soft matter consisting of a three-dimensional cross-linked network of hydrophilic insoluble polymers (hydrogelators) with water as the dispersion medium.[1] With a significant amount of water in the network，hydrogels exist in a half liquid-like and a half solid-like state[2] and thereby possess high water storage capacity, elasticity, flexibility, and permeability.[3] The network structure in the hydrogels can be formed by either chemical cross-linking or physical cross-linking.[4] The physically cross-linked hydrogels are formed through micro-crystallization or entanglement of polymer chains with non-covalent bonds, including electrostatic interaction, hydrophobic interaction, hydrogen bonding, and coordination bonds. Scientific studies have proved that hydrogels can also be produced from the supramolecular assembly of amphiphilic organic molecules[5] or inorganic nanoparticles[6] in water. Some physical hydrogels can undergo a sol-gel phase transition (SGPT)[7] as a response to external stimuli.[8,9] By contrast, the chemically cross-linked hydrogels are permanent networks through covalent bonds, enabling volume phase transitions (VPT)[10] when exposed to external physical or chemical stimuli, which include temperature,[11,12] light, electric field,[13] ionic strength,[14] pH,[15] enzyme,[16] and biomolecules. As a result of these characteristics, hydrogels can be used as superabsorbents,[17,18] packaging materials,[19] soft lenses,[20] microfluidic devices,[21] catalyst supports,[22,23] biomedical materials[24,25] and bioactuators[26] (**Fig. 1a**).

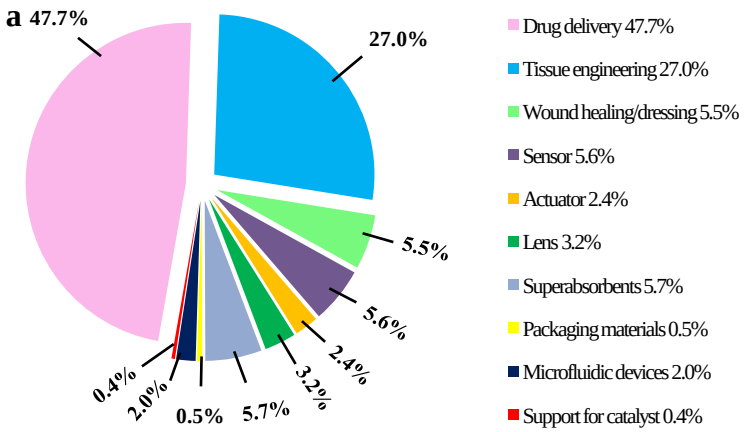

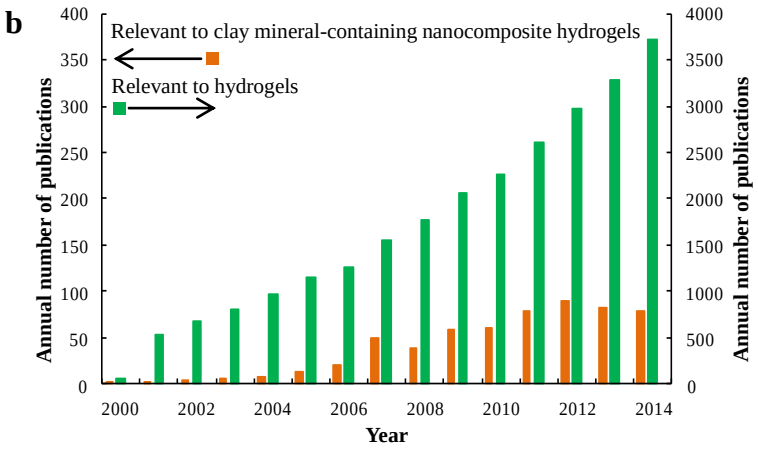

Fig. 1. a) Application category distribution of hydrogels (by percentage) according to peer-reviewed scientific papers published (from 2000 to end of 2014) relating to the topic of hydrogels. b) Annual number of peer-reviewed papers published (from 2000 to 2014) relevant to the topics of hydrogels and clay mineral-containing nanocomposite hydrogels. (Data from Web of Science™ Core Collection. Search terms: hydrogels and clay).

Hydrogel-forming insoluble polymers or amphiphilic organic molecules and inorganic nanoparticles can be assembled to form nanocomposite hydrogels. One of the frequently used nanoplatelets (NPs) is two dimensional (2D) nanomaterials such as layered clay mineral nanoplatelets (CNPs)[27,28] and layered double hydroxide （LDH） nanosheets[29]. Due to the significant effects of CNPs on the structure and properties of polymer/CNPs nanocomposite hydrogels, such nanocomposite hydrogels have captured particular attention over the past decade or so with a rapid growth in the number of relevant scientific publications (**Fig. 1b**). Smectitic clay minerals (**Fig. 2**), in particular natural montmorillonite and synthetic hectorite (e.g., laponite®), are often used owing primarily to their layered structure and unique properties. Each TOT layer of the clay minerals consists of one Al-O or Mg-O octahedral (O) sheet sandwiched by two Si-O tetrahedral (T) sheets, with negative charges arising mainly from the partial isomorphous substitution, typically Al^{3+} by Mg^{2+} in montmorillonite, and Mg^{2+} by Li^{+} in hectorite in the octahedral sheet.[27,28] For this reason, exchangeable cations such as Na^{+} exist in the interlayer space. Such structure makes these clay minerals possess outstanding cation exchangeability, adsorption and swellability. Importantly, these layered clay minerals can be fine-exfoliated to yield nanoplatelets[30] with a high aspect ratio (e.g., approximately $100 \times 100 \times 1$ nm^3 for montmorillonite[31]). Though such exfoliated clay minerals in water can form a physically cross-linked hydrogel, this unique feature of polymer/clay mineral nanocomposite hydrogels received little attention until 2002 when a pioneering study from Haraguchi and Takehisa[32] unveiled a unique poly(*N*-isopropyl acrylamide) (PNIPAM)/clay mineral nanocomposite hydrogel. The nanocomposite

hydrogel exhibited extraordinary mechanical, optical, and swelling/deswelling properties. Since then, a variety of clay mineral-containing nanocomposite hydrogels have been reported. These studies have indicated that when such 2D CNPs are added to a polymeric hydrogel matrix, additional interactions take place between the CNPs and polymers, resulting in creation of nanocomposite hydrogels with improved mechanical properties,[33-35] stimuli-responsiveness,[36,37] swellability,[38] and self-healing abilities,[39] compared to the hydrogels consisting of single hydrophilic polymers.

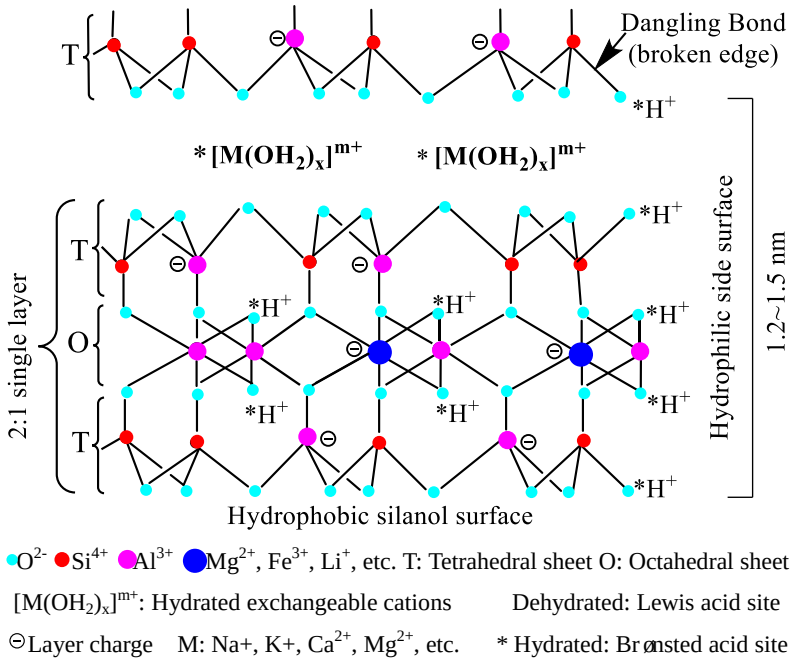

Fig. 2. The schematic drawing of the structure of the frequently used 2:1-type (TOT-type) layered smectite minerals in nanocomposite hydrogels. Each layer consists of an octahedral alumina/magnesia sheet sandwiched by two tetrahedral sheets of silica through sharing -O-. Neighboring layers are loosely bound with counter ions (typically sodium or calcium) in the interlayer space. The interlayer space is the space between adjacent layers. In the presence of water, the counter ions hydrate, causing the clay mineral to expand and delaminate.

This paper intends to review and analyze recent advances in clay mineral-containing nanocomposite hydrogels with an objective to highlight the state-of-the-art technologies used in the preparation of clay mineral-containing nanocomposite hydrogels. Another objective of this paper is to examine the current understanding of the effects of clay mineral additives on polymer/clay hydrogel network formation, properties, and applications. The third objective is to identify the existing challenges that may steer future work in this field. First, the exfoliation of layered clay minerals is overviewed. Then, the formation of polymer/clay mineral nanocomposite hydrogels and inherent interactions in the network are discussed. Next, the characteristics of the clay mineral-containing

nanocomposite hydrogels in optical and mechanical properties, swelling-deswelling behavior, and stimuli-responsiveness are analyzed, with particular focus on the effects of clay mineral nanoplatelets on the properties. Subsequently, the performance of hydrogels and their potential applications as superabsorbents and biomaterials are evaluated with respect to the specific constituent clay minerals. Finally, the existing problems and prospects are remarked.

2. Insights into formation of nanocomposite hydrogels

2.1. Exfoliation and addition of clay minerals into polymeric hydrogel networks

Two-dimensional CNPs can act as multifunctional cross-linkers [40, 41] or fillers [42] in the nanocomposite hydrogels. As far as the role of clay minerals as an enhancement nanophase in the nanocomposite hydrogels is concerned, to achieve and utilize CNPs from the exfoliation of clay mineral tactoids is a critical issue. For most of clay minerals, due to their greater layer charge densities (e.g., vermiculite, 1.1-2.0 electronic charges/per unit cell) or electrically neutral layers (e.g., kaolinite), the exfoliation is difficult. By contrast, montmorillonite and laponite are composed of several parallel TOT layers, and the negative charge per unit cell from isomorphic substation ranges between 0.5 and 1.3 electronic charges. Their parallel TOT layers, which are usually packed one above the other with the exchangeable hydrated cations located between the layers, can be essentially exfoliated by proper treatments (**Fig. 3)**. When water and polar organic molecules are attracted by the exchangeable cations and are intercalated in the layers, the structure expands in a direction perpendicular to the layers.

For the delamination of layered montmorillonite and laponite to form exfoliated CNPs, the electrostatic forces between the negatively charged layer and interlayer cations must be overcome. In addition, the swelling of the layered structure depends heavily on the exchangeable cation or intercalated species in the interlayer space. Hence, easily hydrated cations (e.g., Na^+)[43] and bulky organic cations[44] are introduced into the interlayer space by ion exchange reaction (**Fig. 3a)**. Moreover, for an effective exfoliation, the use of a dilute aqueous suspension of clay minerals is imperative. Besides, the exfoliation process is usually conducted with the aid of sonication[45] and by using exfoliating agents like pyrophosphate[46] and polymeric species[47]. For example, Guimaraes et al.[46] exfoliated laponite, and obtained a transparent laponite suspension (20 g L^{-1}) by mixing 3.6 g of

laponite with 180 mL of an aqueous solution of tetrasodium pyrophosphate (1 g L^{-1}) under stirring for 30 min. Mongondry et al.[48] revealed that tetrasodium pyrophosphate was adsorbed onto the positively charged edges and restrained the interaction between the edges and the negatively charged surfaces of the laponite, thereby hindering the reaggregation of exfoliated CNPs. In particular, the monomer, a precursor of hydrogel-forming polymer, is used to help the exfoliation and to stabilize the CNPs.[49] Consequently, materials consisting of CNPs with monomer can be directly used in the subsequent *in-situ* free radical polymerization. The exfoliation and stabilization of CNPs can also be achieved by polymeric species such as polyethylene oxide (PEO)[48] or polyamine salts (**Fig. 3b**). For instance, Chu et al.[47] synthesized hydrophobic POP-AMO polyamines (POP: polyoxypropylene; AMO: amine-terminating Mannich oligomers) for the Na^+-montmorillonite exfoliation. Such POP-segmented quaternary salts can undergo an ionic exchange reaction with Na^+ of montmorillonite and, consequently, expand the montmorillonite into the exfoliated CNPs. Recently, Wang et al.[50] also exfoliated the pristine multilayered sodium montmorillonite into individual nanoplatelets using polyamine quaternary salts. The platelet-to-platelet multilayers of montmorillonite were completely exfoliated. The exfoliated platelets could then be extracted with two-phase toluene/NaOH to remove the organic exfoliating agents.

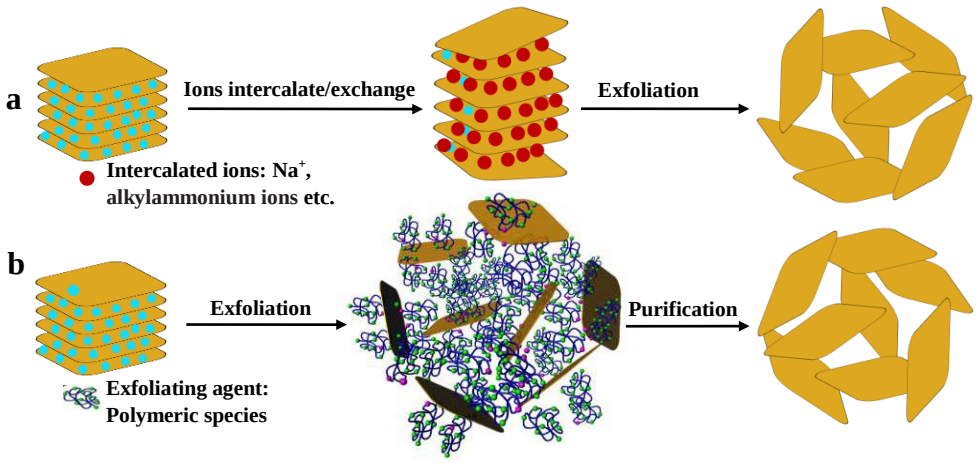

Fig. 3. Techniques for exfoliating clay minerals: a) easily hydrated cations or bulky ion intercalation/exchange. Bulky cations can be intercalated in the interlayer space to cause the layered structure to swell and exfoliate. b) Using polymeric species as exfoliating agent. These exfoliation processes are often used with aid of sonication. Adapted and reprinted by permission from Macmillan Publishers Ltd: [NATURE] (reference 50), copyright (2013).

The exfoliated CNPs usually in the form of an aqueous suspension have been successfully introduced into various polymer networks to form nanocomposite hydrogels (**Fig. 4**). The typical

approaches are the *in situ* free radical polymerization, supramolecular assembly, and the freezing-thawing cycles. For the *in situ* free radical polymerization, the CNPs suspension can be added and well mixed with the aqueous solutions of nonionic monomers, such as acrylamide (AM)[51] or acrylamide derivatives, *N*,*N*-dimethylacrylamide (DMA) and *N*-isopropylacryamide (NIPAM)[52]. Moreover, in the polymerization of ionic monomers, such as acrylic acid (AA),[53] sodium methacrylate (SMA),[54] sodium 4-styrene sulfonate (SSNa) or 2-acrylamido-2-methylpropane sulfonic acid (AMPS), the charged CNPs were pre-adsorbed onto the monomers to avoid aggregation of exfoliated CNPs. Well-exfoliated CNPs can also be introduced into the pre-prepared polymeric hydrogel networks of poly(ethylene glycol) (PEG),[55] sodium polyacrylate (PAAS)[56] or poly(*N*-vinyl-2-pyrrolidone) (PVP)[57] to form hydrogels. In addition, exfoliated clay minerals can be mixed with pre-designed macromolecules in water to obtain clay mineral-containing nanocomposite hydrogels by supramolecular assembly.[58] Moreover, the mixture of exfoliated clay minerals or organically modified clay minerals and hydrophilic polymers (e.g., poly(vinyl alcohol), PVA) and oligomers (e.g., poly(ethylene glycol) diacrylate, PEGDA) can form clay mineral-containing nanocomposite hydrogels by the treatment of the freezing-thawing cycles.[59,60]

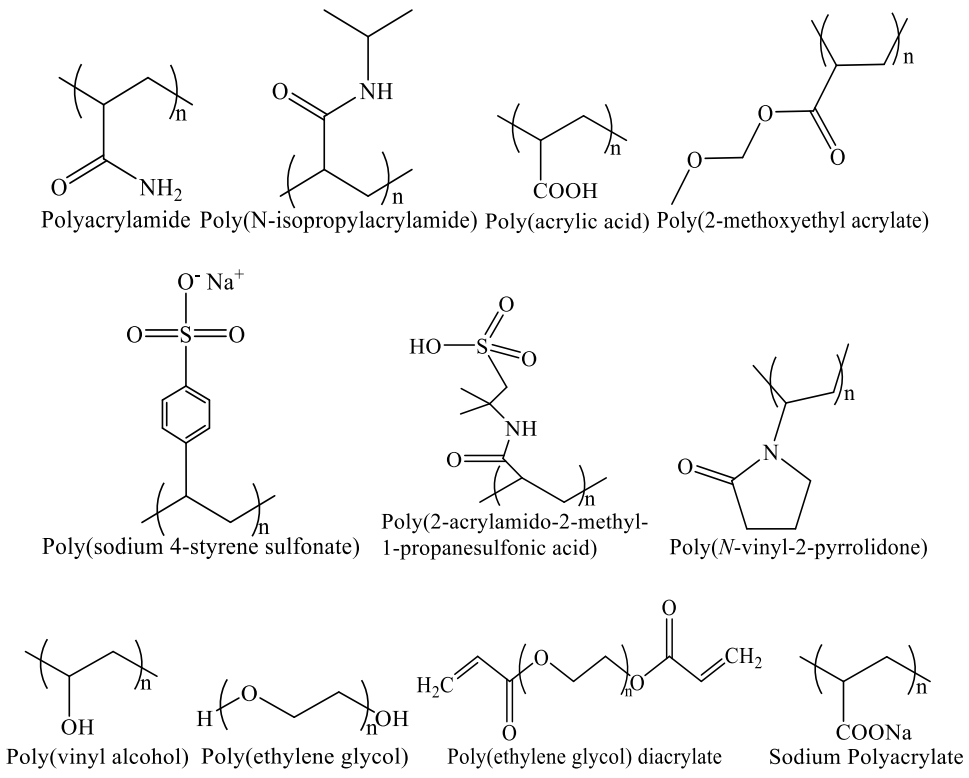

Fig. 4. The polymers frequently used in forming clay mineral-containing nanocomposite hydrogels.

2.2 *In-situ* free radical polymerization

In-situ polymerization is one of the most common methods for preparing nanocomposite hydrogels because the types of nanofillers and polymer precursors can be varied in a wide range to achieve desired properties **(Table 1)**. In the *in-situ* free radical polymerization, exfoliated CNPs are pre-prepared and mixed with an aqueous monomer solution to achieve a homogeneous dispersion of the CNPs throughout the polymer matrix. The polymerization reaction is then initiated by external stimuli such as thermal, photochemical, or chemical activation through initiators and/or catalysts and proceeds *in-situ* on the surface of CNPs **(Table 1, Fig. 5a)**. Under such circumstances, both chemically cross-linked polymeric network and physical entanglement of the polymer chains can be formed with CNPs distributed inside the network.[61] In other words, in the network, covalent interactions occur between neighboring polymeric molecules. It is also possible to form covalent bonds between the surface hydroxyl groups of CNPs and polymeric molecules. Also, non-covalent interactions including hydrogen bonding, electrostatic interactions, coordination bonds and hydrophobic interaction, namely physical cross-linking could exist in these nanocomposite hydrogels.[62,63] However, the quantification of these chemical and physical interactions remains difficult.

As summarized in Table 1, the *in-situ* polymerization is often initiated by chemical initiators[64] such as ammonium persulfate, potassium persulfate, and benzoyl peroxide (BP), depending upon the reaction. For example, Okay et al.[65] used ammonium persulfate as a redox initiator for the polymerization of AM in the presence of laponite CNPs, and produced polyacrylamide (PAM)/laponite nanocomposite hydrogels. Shen et al.[66] used potassium persulfate (KPS) as an initiator for polymerizing AA and obtained poly(acrylic acid (PAA)/laponite nanocomposite hydrogels. In these hydrogels, in addition to intermolecular interactions between polymeric chains, laponite NPs served as cross-linkers between PAA chains. Such additional interactions contributed by CNPs become more complicated in the case of copolymerization. For example, a small amount of BP was used as initiator in the preparation of nanocomposite hydrogels by grafting linear low density polyethylene (LLDPE) on AA, to form LLDPE-*g*-PAA/montmorillonite superabsorbent hydrogels.[67] In such a network,

interactions between the -COOH or -COO^- groups of AA and -OH groups of montmorillonite NPs are conceivable. Montmorillonite NPs specifically are utilized as multifunctional cross-linkers. As a result, a more stable and homogeneous hydrogel network was achieved relative to the single chemically cross-linked polymeric hydrogels without CNPs as cross-linkers.

Table 1. The Clay Mineral-Polymer Nanocomposite Hydrogels Synthesized by *in-situ* Free Radical Polymerization

Monomer	Clay mineral	Additives	Condition	Property	Reference
AM	Laponite RD; Laponite RDS	TEMED; KPS: 20 mg/mL	30℃ 72 h	Elongation: > 4000%; Strength: 110 kPa; Relaxation modulus: ~0.16	51
AM: 3 g	Laponite XLS: 0.5–2 g	TEMED: 24μL; KPS: 20 mg/mL	30℃ 48 h	Adsorption of CV dye increased with increasing laponite concentration	68
NIPAM: 0.03 g	Laponite XLG: 0.198-1.782 g	TEMED: 24μL; KPS: 20 mg/mL	20℃ 20 h	Elongation: ~1,000%; Swelling/deswelling; Transparency	69
SSNa: 5.00 g; AAG 5.00 g	APTMA-MMT	APS	70℃ 4 h.	Thermal stability: up to 400℃; absorbability	70
AA: 7.20 g	CTAB-illite/smectite: 0.235 g	APS: 0.10 g; styrene: 0.15 g; NMBA: 0.0216 g; sodium alginate: 1.20 g	70℃ 3 h.	Absorbability of methylene blue: 1843.46 mg/g	71
AMPS: 30.0 g	Chitosan: 1.0g – MMT:4.0 g	APS: 0.15 g; PEGDMA: 0.24 g	70℃	Absorbability: 440 g/g; thermal stability: up to 434℃ glass transition temperature: ~98.2℃; Elastic modulus: 238%	72,73
AA: 5-13 g	ODA-MMT: 0.30-1.10 g	Span 60: 0.3 g; BP: 0.03-0.05 g; NMBA: <0.01 g	70℃ 3 h	Absorbability in distilled water: 800 g/g; absorbability in saline solutions: $M^+ > M^{2+} > M^{3+}$ decomposition with increasing temperature.	67
AM	Bentonite	NMBA; APS	Sonication assisted	Swelling/deswelling	74
AM: 3 g	Halloysite: 6 g	KPS: 3 ml	65℃ 18 h	Swelling ratio:4,000%	75
Acryloyl chloride	Laponite XLS	PEG; Irgacure 2959	UV irradiation λ=365 nm, 45 $mWcm^{-2}$; 5 min	Compressive modulus: 48.6 kPa; Fracture stress: 3882.8 kPa; Toughness: 268.3 kPa.	60

AA: acrylic acid; AM: acrylamide; AMPS: 2-acrylamido-2-methylpropane sulfonic acid; AAG: acrylamide glycolic acid; NIPAM: *N*-isopropylacrylamide; SSNa: sodium 4-styrene sulfonate; PEG: poly(ethylene glycol); PEGDMA: poly(ethylene glycol) dimethacrylate.

APS: ammonium persulfate, BP: benzoyl peroxide used as initiator, and KPS: potassium persulfate as initiator; APTMA: (3-acrylamidopropyl) trimethylammonium, CTAB: cetyltrimethylammonium bromide and ODA: octadecylamine as organic modifier; MMT: montmorillonite; NMBA: *N,N*-methylene-(bis)-acrylamide as cross-linker; TEMED: *N,N,N',N'*-tetramethylene diamine used as catalyst/accelerator; TSPP: tetrasodium diphosphate decahydrate used as dispersing agent; CV: crystal violet.

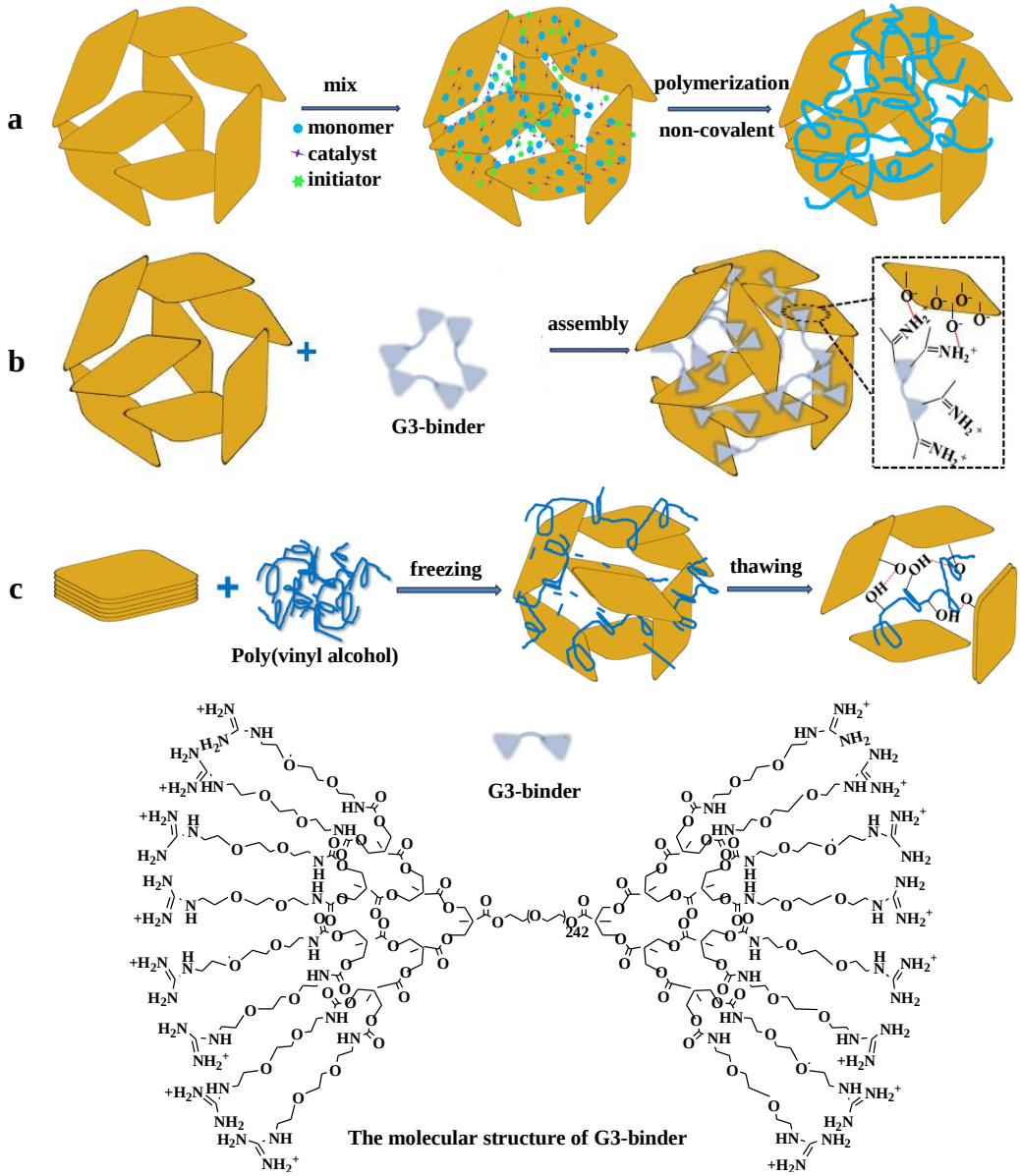

Fig. 5. Three methods to prepare clay-containing nanocomposite hydrogels. a) *In situ* free radical polymerization usually starting from the mixture of monomer, catalyst, and initiator under room temperature; b) Supramolecular assembly through the direct mixing of clay minerals with pre-designed dendritic macromolecule, G3-binder, which carries adhesive dendron units at both termini of a long, hydrophilic polyethylene glycol (PEG) spacer. Adapted and reprinted by permission from Macmillan Publishers Ltd: [NATURE] (reference 58), copyright (2010); and c) freezing-thawing cycles, starting from a mixture of poly(vinyl alcohol) (PVA) and clay minerals.

Apart from polymerization initiated by chemical initiators, in the presence of a photoinitiator, polymerization can be initiated and facilitated by taking advantage of radiation (electron beam or γ photon). As such, the *in-situ* polymerization in the solution of mixed CNPs and monomers can be conducted at mild or room temperature.[76] In addition, the photopolymerization initiated using ultraviolet light or visible light is faster than that of polymerization using photochemical initiators.[60] Moreover, photoinitiated free radical polymerization offers an advantage of solvent-free formulation over thermally initiated free radical polymerization. For instance, using 1-hydroxy-cyclohexyl-phenylketone (Irg. 184) as photoinitiator, Haraguchi et al.[77] prepared PNIPAM/laponite nanocomposite hydrogels by free radical polymerization under a 365 nm of UV light for 3 min. This method provided an efficient way of producing hydrogels in which uniformly dispersed laponite NPs act as multifunctional cross-linkers, similar to that in the polymerization initiated by chemical initiators. It is worth pointing out that CNPs can be modified with photoinitiator beforehand, and the resultant hybrid can function to initiate the photopolymerization and to provide CNPs *in situ*.for the resultant polymeric networks[78]

2.3 Supramolecular assembly

Direct mixing of macromolecules with clay minerals in water is a new facile route to produce nanocomposite hydrogels. Nevertheless, the macromolecules require functional groups that can directly cross-link with nano-sized clay mineral platelets in water. As demonstrated by pioneering work by Wang et al.,[58] a supramolecular nanocomposite hydrogel was obtained by directly mixing well-designed dendritic macromolecules with laponite NPs (**Fig. 5b**). The interactions between functional groups on the peripheries of dendritic macromolecules and the surface of CNPs led to a novel supramolecular assembly. Thus, a high-water-content mouldable hydrogel was achieved. Interestingly, in this process, mixing water and laponite (2–3 wt%) with a very small proportion (< 0.4 wt%) of organic components produced a transparent hydrogel. No catalysts or initiators were required for this assembly compared with the *in situ* free radical polymerization. Nonetheless, exfoliation of clay minerals and homogeneous dispersion of CNPs in water and the surface functional groups of the macromolecules are two critical factors. Hence, the laponite can be effectively dispersed with the pre-treated sodium polyacrylate.

In addition, the dendritic structure of the macromolecules is critical in forming a supramolecular

hydrogel network with dispersed CNPs in it. It was proved that the multiple guanidinium ion pendants of dendritic macromolecule connected with oxyanions on the surface of CNPs through salt-bridge formed by electrostatic interaction. Though the nanocomposite hydrogel was formed merely by non-covalent forces resulting from the specific design of a telechelic dendritic macromolecule with multiple adhesive termini for binding to clay, they show high mechanical strength, and rapidly and completely self-healing when damaged and consequently be moulded into shape-persistent, free-standing objects. Based on such methodology, the well-designed linear macromolecules with proper surface functional groups can also cross-link with CNPs through salt-bridge to form nanocomposite hydrogels. For example, Tamesue et al.[79] mixed linear macromolecule with laponite XLG NPs, which are pre-dispersed in water with a minute amount of sodium polyacrylate. In this way, a supramolecular nanocomposite hydrogel composing of linear macromolecule and laponite XLG NPs can successfully be obtained. Similarly, it was believed that salt-bridge between the guanidinium ion in the terminal of linear macromolecule and the oxyanions on the surface of laponite NPs mainly contributed to the formation of such a hydrogel with a well-defined cohesive structure.

Comparatively, the linear macromolecules are less expensive than dendritic macromolecules. It is noteworthy that at sufficiently high concentrations and under electrostatic screening conditions, charged supramolecular polymers can easily produce a three dimensional (3D) network that takes the form of a hydrogel. Therefore, it is possible that such method could be applied to many other molecules with the CNPs. In particular, a recent study revealed that small organic molecules can also form a supramolecular hydrogel through such supramolecular assembly and micro-crystallization.[80] Yet, whether the assembly to form the small organic molecule-based hydrogel works in the presence of CNPs is relatively unknown.

2.4 Freezing–thawing cycles

In addition to polymerization and supramolecular assembly**,** a physical cross-linking method can also result in the formation of an entangled, cross-linked hydrogel network.[81] It has been found that a freezing–thawing process of a mixture of polymer with clay minerals in water can facilitate the incorporation of clay minerals into the polymer networks. PVA is particularly suitable to be used with clay minerals to form physically cross-linked hydrogels by freezing-thawing cycles.[82,83]

Typically, PVA and montmorillonite are mixed in distilled water and heated to achieve complete dissolution.[84] Then the aqueous solution consisting of clay minerals and polymers undergoes a freezing process normally at -20 ℃, subsequently with thawing at room temperature in air. Repeating such a freezing–thawing operation results in the formation of nanocomposite hydrogel with dispersed CNPs in it (**Fig. 5c**). The presence of clay minerals in the three dimensional network of a hydrogel causes an increase in cross-linking density, thus creating a more entangled structure.[84] Ibrahim and El-Naggar[85] also found that freezing-thawing cycles facilitated the entanglement of PVA chains, and further proved that the freezing-thawing cycles can drive cross-linking through hydrogen bonds between the hydroxyl group of PVA chains and oxyanions on the surface of montmorillonite. Thus, physically cross-linked hydrogels with ability to undergo sol-gel transition exhibited thermo-reversible performance. In addition, the resultant hydrogels exhibited high thermal stability by increasing clay content in the hydrogels. It is worth noting that in the freezing and thawing process, there is no need for any additional chemical or elevated temperature. Interestingly, the freezing and thawing techniques can be employed with electron beam (EB) irradiation to produce PVA/clay hydrogel.[85]

3. Effects of clay minerals on the properties of nanocomposite hydrogels

The mechanical and thermal properties of the nanocomposites can be significantly enhanced when nano-sized platelets of clay minerals are uniformly dispersed in the polymer matrix.[86] The similar enhancements are also achieved when such clay minerals are incorporated into polymeric hydrogels. The exceptional toughness obtained through clay mineral addition in nanocomposite hydrogels,[32] is attracting increasing research on this material in the last decade. In addition, loading of CNPs into the polymeric hydrogels can alter the optical transparency and anisotropy, swelling-deswelling and stimuli-responsiveness. Superficially, the effects of clay minerals on the properties of nanocomposite hydrogels are dependent on; (1) the type of clay minerals (e.g., the 1:1 type and the 2:1 type); (2) the concentration of CNPs in the network; (3) the dispersion degree of CNPs in the network structure. However, the physical and chemical interactions between polymers and CNPs are of paramount importance.[87,88]

3.1 Optical property

Hydrogels with high optical transparency are paving way for innovations such as transparent wound dressing with optical clarity for facile wound inspection[89] and sensors with optical response (transparency and optical anisotropy) vary with external stimulus such as a temperature change.[90,91] The addition of clay minerals into the polymeric hydrogels can hence be used to tune the optical transparency of the nanocomposite hydrogels. The optical transparency is related to the uniform structure in the nanocomposite hydrogels.[92] Remarkably, the PNIPAM/laponite nanocomposite hydrogels have high transparency regardless of the concentration of laponite in a range of 1×10^{-2} mol/L to 25×10^{-2} mol/L.[93] When the concentration of laponite is lower than 10×10^{-2} mol/L, the PNIPAM nanocomposite hydrogels show a sharp decrease in transparency at their lower critical solution temperature (LCST).[94] When the concentration of laponite is higher than 10×10^{-2} mol/L, the transparency remains constant regardless of the LCST, because the thermal-molecular motion of the polymers is completely restricted by exfoliated laponite nanoplatelets in the network of nanocomposite hydrogels.

CNPs can affect ordering and the crystallization behavior of polymers as well, leading to changes in optical anisotropy. Murata and Haraguchi[95] revealed that for nanocomposite hydrogels with PNIPAM/laponite XLG network structures, the optical anisotropy exhibited unique changes when the nanocomposite hydrogels were deformed uniaxially. The optical anisotropy of clay mineral-containing nanocomposite hydrogels can be measured by birefringence phenomena. The birefringence phenomena of nanocomposite hydrogels correlate with the orientation of polymers and CNPs in the network structure[95], where the distinct maxima and sign inversions are indicative of strain and hydrogel composition **(Fig. 6a)**. Such PNIPAM/laponite XLG nanocomposite hydrogels, present ordered structure on uniaxial stretching (**Fig. 6b**), and exhibit strong birefringence due to optical anisotropy.[96] In the unstretched, isotropic state **(Fig. 6c),** however, PNIPAM chains and CNPs are randomly oriented in the nanocomposite hydrogels, resulting in non-birefringence. In addition to polymer chains, the alignment of CNPs in aqueous colloidal dispersions is subjected to an external force, and thereby induces a structural ordering and CNPs separation and distribution.

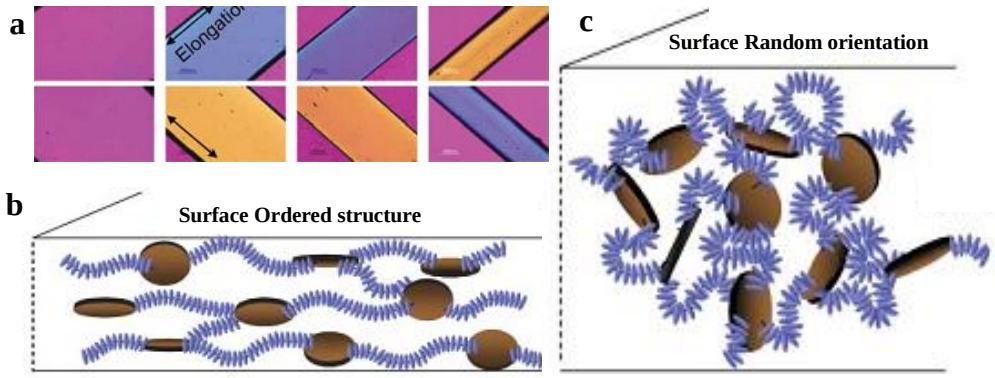

Fig. 6. a) Polarized-light micrographs (a-d) of stretched nanocomposite hydrogels consisting of poly(*N*-isopropylacryamide) PNIPAM and laponite XLG at strain of 0%, 300%, 740% and 1300%, respectively. Test is conducted under crossed polarizers in conjunction with a 530 nm retardation plate, where + 45 °(-45 °) orientation is parallel to the slow (fast) axis of the retardation plate. b) The stretched state of nanocomposite hydrogels. c) The unstretched state of nanocomposite hydrogels. PNIPAM chains and clay platelets are randomly oriented in the nanocomposite hydrogels being non-birefringent. Adapted and reprinted from {Reference 95} with permission of The Royal Society of Chemistry.

3.2 Mechanical properties

The mechanical properties of pure polymeric hydrogels are typically lower, compared with hydrogels with reinforcement nanoparticles where inorganic fillers offer additional adhesion with a polymer matrix. In contrast to 1D or 3D nanoparticles, negatively charged lamellar clay nanosheets embedded within polymeric networks enable the hydrogels to exhibit much exceptional mechanical properties. Earlier, Haraguchi et al.[34] investigated the PNIPAM/laponite nanocomposite hydrogels with the concentration of laponite up to 25 $\times 10^{-2}$ mol/L H_2O. The resultant hydrogels exhibited remarkable increases in tensile strength (1.1 MPa) and modulus (453 kPa). These clay mineral-containing nanocomposite hydrogels interestingly can be elongated to more than 1000% of their original length.[97] The enhanced tensile behavior of the clay-containing nanocomposite hydrogels is attributed to the unique network of uniform cross-linking between CNPs and the long, flexible polymer chains. In particular, the homogeneous dispersion of clay nanoplatelets into polymer network at a nanometer scale can assist in obtaining a narrow length distribution of polymer chains, and subsequently result in superior tensile behaviors of the nanocomposite hydrogels.

The increased tensile strength and modulus are attributed to the additional physical and/or chemical interactions among polymers, colloidal CNPs, and water. Chang et al.[60] prepared PEGDA/laponite nanocomposite hydrogels with enhanced mechanical properties by harnessing the

ability of PEGDA oligomers to simultaneously form chemically cross-linked networks while binding with laponite nanoparticles through secondary interactions.

The significant enhancement of the compressive and tensile properties of PEGDA hydrogels was primarily ascribed to incorporation of laponite nanoparticles, and affected by the molecular weight of PEG and concentration of laponite nanoplatelets. Hence, the synergistic interactions become more complicated because of the presence of CNPs in the polymeric networks, which play a key role in the mechanical behavior of the nanocomposite hydrogels.[98] At present, the inherent reasons for the exceptional toughness of clay nanocomposite hydrogels remain elusive, and necessitate further investigation. In addition, clay minerals can improve the hydrophilicity and flexibility of networks resulting in increases in tensile strength and the modulus.[99]

Similarly, the compressive strength and modulus increase almost proportionally to the concentration of clay minerals, but such a conclusion is simply applicable to the cases in which a specific type of CNPs and its amount in a certain range are used (e.g., for laponite, lower than 25×10^{-2} mol/L).[100,101] In the case of the addition of laponite CNPs, at concentrations below 10×10^{-2} mol/L-H_2O, 90-99% recovery from elongation of 900% was achieved. When the concentration was higher than 10×10^{-2} mol/L-H_2O, the recovery decreased significantly with an increasing concentration of laponite.[102] Considering CNPs are a class of negatively charged lamellar nanoplatelets, a recent breakthrough on nanocomposite hydrogel using negatively charged unilamellar titanate nanosheets is worth discussion.[103] It was found that a strong magnetic field can induce co-facial nanosheet alignment in aqueous colloidal dispersions, which can maximize electrostatic repulsion, and thereby induce a quasi-crystalline structural ordering over macroscale along with uniformly large face-to-face nanosheet separation. This transiently induced structural order can be tactically fixed by transforming the dispersion into a hydrogel using light-triggered *in situ* vinyl polymerization. The resultant hydrogel containing charged inorganic structures can align co-facially in a magnetic flux deform easily under shear forces applied parallel to the embedded nanosheets, yet resisting compressive forces applied orthogonally. These findings clearly reveal that soft materials using 2D nanoparticles can lead to unique functions.

3.3 Swellability

Swellability and delamination are characteristic of clay minerals such as montmorillonite, hectorite and synthetic laponite. These properties are comparable with the swellability of certain polymeric hydrogels. The nanocomposite hydrogels consisting of water-swellable clay minerals, e.g., laponite or montmorillonite exhibit peculiar swellability, including high swelling rate, large, but finite equilibrium swelling ratio and spontaneous deswelling in water.[104,105] For example, Zhang et al.[106] reported that a PAA/montmorillonite nanocomposite hydrogel showed a higher swelling ratio than their corresponding clay-free hydrogels. It was suggested that montmorillonite NPs helped to form a highly loose and porous structure in the nanocomposite hydrogels, and thereby improved the swelling ratio of the PAA/montmorillonite nanocomposite hydrogels.[107] Firstly, the polymer chains in the unique network structure will be more flexible for swelling when physically cross-linked by CNPs, as opposed to pure chemically cross-linking polymer network. Secondly, the increment of swellability can be attributed to the increased ionic osmotic pressure resulting from the mobile ions on the surface of clay minerals and the hydrated cations in the interlayer. Due to the negative charge on the surface of CNPs, sodium counterions are uniformly dispersed in the network of hydrogels. The hydrogels consequently swell in pure water allowing water molecules to enter into the network and diffusion of mobile sodium ions from the network until reaching an equilibrium swelling state (**Fig. 7**). The swelling state was dependent upon the release of sodium ions, and the deswelling of the nanocomposite hydrogels appeared spontaneously. The swelling-deswelling behavior is apparent in the network structure of nanocomposite hydrogels consisting of nonionic polymer PAM and laponite RD.[108] It has been observed with swelling that a substantial volume of water is entrapped within the hydrogels, because of osmotic pressure changes and free ions movement between the hydrogels and solution. The hydrogels can swell to an equilibrium state, during which the outflow of mobile ions leads to a low ionic osmotic pressure and subsequently, deswelling. It is noteworthy that such increment is also caused by CNPs used in hydrogels. For instance, Darvishi et al.[109] obtained a maximum swelling ratio for poly(AMPS-*co*-*N*-[3-(dimethylamino)propyl] methacrylamide (DMAPMA))/bentonite anionic-cationic nanocomposite hydrogels with 10.2 wt% of nanobentonite. Kaşgöz et al.[110] drew a similar conclusion for poly(2-acrylamido-2-methylpropane sulfonic acid) (PAMPSA)/laponite nanocomposite hydrogels, where laponite in fraction greater than 10 wt% in hydrogels resulted in a lower swelling ratio. For instance, with the content of 10 wt% laponite, the nanocomposite hydrogels reached to the maximum

swelling ratio (164.3 g water/g sample). The increase of the concentration of CNPs led to higher cross-linking density in the network structure.[111,112] By further increasing the concentration of CNPs, the reduction of swelling ratio appeared, owing to the higher cross-linking density in the network structure, which could not be expanded easily.[113]

Similar phenomena were observed when laponite was utilized for PNIPAM/laponite nanocomposite hydrogels,[114] and attapulgite was used for PAA/attapulgite nanocomposite hydrogels[115]. In comparison to attapulgite, kaolinite, and mica, PAM/Na^+-montmorillonite nanocomposite hydrogels exhibited a higher swelling rate in distilled water.[116] Zhang and coworkers[116] compared the effects of different kinds of clay minerals, with a concentration of 10 wt% of montmorillonite, attapulgite, and kaolinite on the swelling behaviors of the PAA-based hydrogels in a cationic saline solution.[117] The PAM/attapulgite nanocomposite hydrogels showed the highest swelling ratio in NaCl solution. In $FeCl_3$ solution, the PAM/kaolinite nanocomposite hydrogels exhibited the highest swelling ratio.

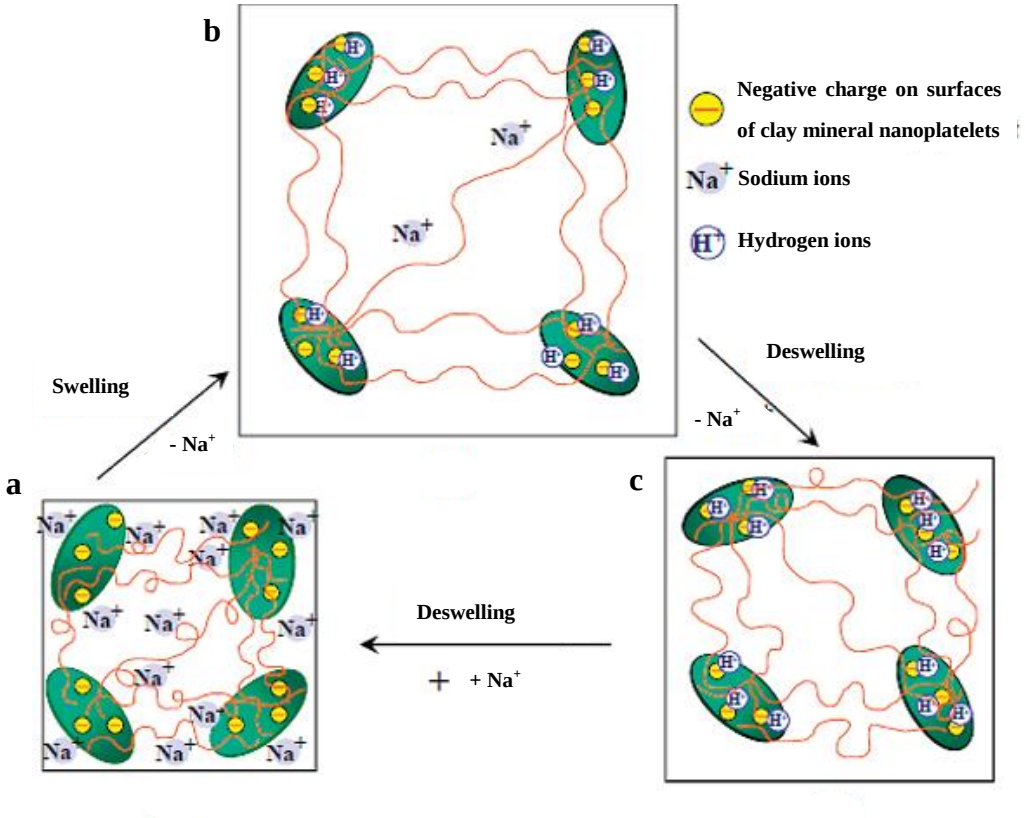

Fig. 7. The swelling-deswelling behavior showing in the network structure of nanocomposite hydrogels consisting of non-ionic polymer poly(*N*,*N*-dimethylacrylamide) (PDMA) and laponite XLG: (a) As-prepared state; (b) Maximum swelling state; (c) Equilibrium swelling state. Only a few polymer chains and counterions are depicted for simplicity. Adapted with permission from reference 105. Copyright (2011) American Chemical Society.

3.4 Stimuli-responsiveness

The stimuli-responsiveness of nanocomposite hydrogels is referred as the phenomena of volume and transparency change reversibly in response to the surrounding stimuli, such as temperature, pH, ionic strength, pressure or electronic field.[118,119] Such properties are of great importance in smart optical materials, diagnostics, biosensors, drug delivery, tissue engineering, coatings and micro-electromechanical systems.

For a given nanocomposite hydrogel, chemically cross-linked networks have permanent connections, while physical networks have transient junctions that arise from either polymer chain entanglements or physical interactions. The use of added CNPs varies with chemically cross-linked networks and physical networks. As a result, CNPs can be used to tune the stimuli-responsive behaviors of nanocomposite hydrogels in volume and transparency.[120] The stimuli-responsiveness of clay mineral-containing nanocomposite hydrogels resulted from the changes in conformation, ordering or solubility of the constituent polymers and CNPs. For example, physically cross-linked clay mineral-containing nanocomposite hydrogels can undergo a SGPT. Typically, a clay mineral-containing nanocomposite hydrogel *in situ* formed by reversible physical networks can readily present reversible sol-gel phase transitions induced by external stimuli. The changes mainly ~~are~~ attribute~~d~~ to the interactions among the polymer chains, CNPs and water, such as hydrophobic interaction, electrostatic interaction and hydrogen bonding. Chemically covalently cross-linked, clay mineral-containing nanocomposite hydrogels have basically permanent networks, which can undergo VPT and changes of optical properties.

On the one hand, CNPs contain hydrophilic edges, with cations in the interlayer space, and hydrophobic silanol surface. Thus, the addition of clay minerals in the polymeric networks could modify the hydrophilic-hydrophobic balance of polymers. As thermo-responsiveness is strictly regulated by the balance of hydrophilic and hydrophobic forces in the network structure, the addition of CNPs affect the thermo-responsiveness of the nanocomposite hydrogels. [121] Typically, thermo-responsive PNIPAM includes both hydrophilic (–CONH–) and hydrophobic (–$CH(CH_3)_2$) groups.[122] PNIPAM chains show thermally triggered conformational change from hydrophilic coil to hydrophobic globular form at LCST (about 32 ℃). The addition of clay minerals can change the

conformation of network structure of the nanocomposite hydrogels, thereby tuning the stimuli-responsiveness. Particularly, the thermally triggered conformational change of polymer chains in clay mineral-containing nanocomposite hydrogels is significantly restricted by clay minerals because of interactions between PNIPAM chains and clay minerals through hydrogen bonding. The PNIPAM chains in the nanocomposite hydrogels exhibit coil-to-globule transition at higher temperatures than normal PNIPAM chains.[123] The thermodynamic balance between hydrophilic and hydrophobic interactions in aqueous media.[124]

On the other hand, the clay mineral-containing nanocomposite hydrogels can gain a better pH-responsiveness in comparison to single-polymer hydrogels, because the conventional hydrogels are cross-linked by small molecules and always show a slower response rate and inferior elasticity.[125] The pH-responsive of hydrogels is usually attributed to their ionic groups. In particular, montmorillonite[126] and laponite[127] are more or less pH-dependent due to the edge charges. The addition of these clay minerals can increase the ionization of polymers following a chain expansion in response to pH. Recently, Li et al.[128] successfully synthesized pH/temperature double responsive nanocomposite hydrogels consisting of poly(DMA-*co*-(2-dimethylamino) ethyl methacrylate (DMAEMA)) cross-linked by laponite NPs. In addition, owing to extra ionic charge provided by CNPs, the incorporation of CNPs into the polymer hydrogels brought about distinct electro-responsive nanocomposite hydrogels with changes.[129] The ion concentration on the surface of CNPs can accelerate the electro-responsive rate whereas the cross-linking density of network in the hydrogels can impede the electro-responsive rate. Such nanocomposite hydrogels containing charged inorganic CNPs may have exceptional changes either in mechanical or optical behavior in response to alternating application and removal of the electric field, arising from the varied alignment of CNPs and polymeric chains.[130]

4. High functional applications of clay mineral-containing nanocomposite hydrogels

4.1 Superabsorbents

A high water uptake is a key characteristic of polymer hydrogels.[131] Clay minerals also have

remarkable adsorption capacity for water and many other inorganic and organic cations. The combination of these two components leads to nanocomposite hydrogels with a much distinct adsorptive behavior. In many cases, smectite clay mineral-containing nanocomposite hydrogels have higher adsorption capacities, faster adsorption rate, and enhanced mechanical stability than polymeric hydrogels.[108,113] Moreover, smectite clay minerals themselves have abundant exchangeable cations in the interlayer space and negative charges on their surface. These performances of clay minerals make the nanocomposite hydrogels to be effective as superabsorbents to remove heavy and toxic metal ions[132] and cationic dyes[133] from the sewage water.

The presence of clay minerals as cation exchangers enables clay mineral-containing nanocomposite hydrogels to possess active sites to adsorb heavy metal ions.[134] The adsorption mainly results from strong electrostatic interactions between smectites and metal ions.[135] In addition, some heavy metal ions can be absorbed by clay mineral-containing nanocomposite hydrogels through coordination bonds, hydrogen bondings or/and dipole association. For example, a study by Guçlu et al.[136] suggested that PAA/montmorillonite nanocomposite hydrogels can be used for the removal of copper (II) and lead (II) ions from water. The adsorption reached to equilibrium within 24 h at pH=4 and room temperature. Ibrahim and El-Naggar[85] prepared PVA/clay nanocomposite hydrogels through freezing and thawing followed by electron beam irradiation for the treatment of wastewater, and revealed that PVA-based hydrogels consisting of 60% of montmorillonite as fillers exhibited a higher adsorption capacity for ions such as Cu^{2+}, Ni^{2+} and Co^{2+} from wastewater.

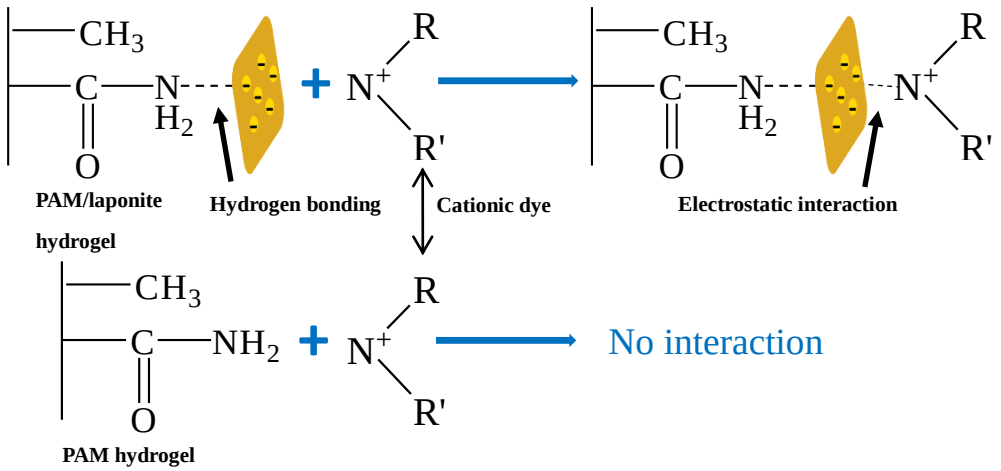

Fig. 8. The mechanism of cationic dye adsorbed by clay mineral-containing nanocomposite hydrogels. The negative charges on the surface of clay mineral (laponite) in nanocomposite hydrogels can readily interact with cationic dye molecules through electrostatic interaction. While, the poly(acrylamide) (PAM) hydrogels without clay minerals could not interact with dyes.

In addition to removal of inorganic heavy metal ions, clay mineral-containing nanocomposite hydrogels can also be used to remove cationic dyes from the wastewater. The adsorption of nanocomposite hydrogel for cationic dyes can be attributed to the electrostatic interaction between anions on the surface of clay minerals and active groups of dyes (**Fig. 8**). Li et al.[68] prepared PAA/laponite nanocomposite hydrogels as superabsorbent materials for adsorbing the monovalent cationic dyes. The dye adsorption rate and equilibrium amount increased significantly with the increased concentration of clay minerals up to 20 wt% in hydrogels. Mahdavinia et al.[137] found that the adsorption capacity of nanocomposite hydrogels composing of kappa-carrageenan, sodium alginate and sodium montmorillonite for cationic crystal violet dyes was to be approximately 2–6 times higher than that of hydrogels consisting of alginate alone. The adsorption rate of the dyes onto alginate nanocomposite hydrogels also increased due to the addition of charged montmorillonite. Besides, the negatively charged surface of clay minerals can be modified by grafting with a variety of functional groups. For example, the surface of CNPs was covalently functionalized with aminopropyl groups to yield aminoclay (AC) **(Fig. 9a)** The AC with aminopropyl groups on the surface was then assembled to form functional hydrogels. Accordingly, the resultant hydrogels were able to absorb anionic dyes such as coronene tetracarboxylate salt and perylene tetracarboxylate salt **(Fig. 9b)**. The increase of adsorption capacity and adsorption rate of dyes onto superabsorbents are affected by both the swellability and porosity resulting from the addition of such clay minerals. For most dyes, the adsorption onto nanocomposite hydrogels correlates well with the Langmuir isotherm equation, and the adsorption kinetics onto the hydrogel composite is consistent with the pseudo-second-order model.[138]

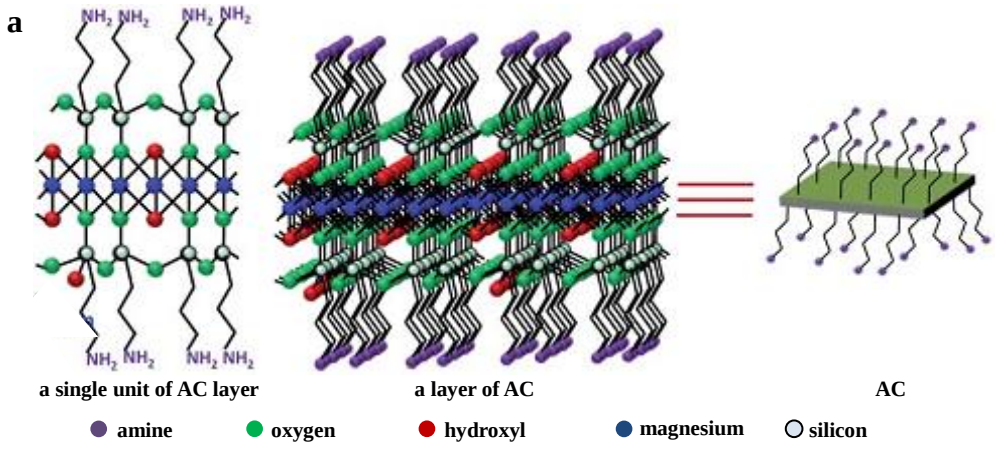

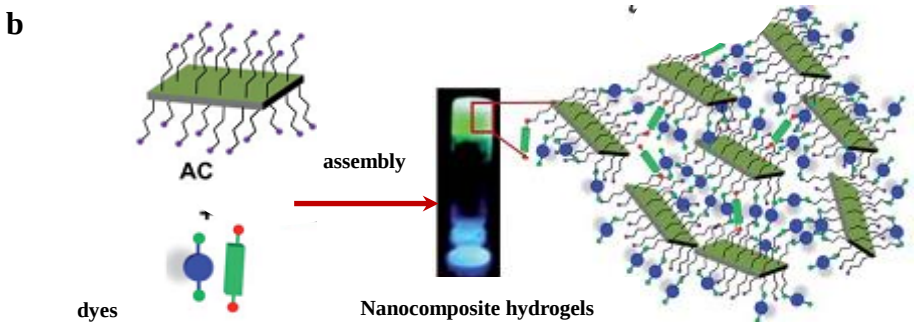

Fig. 9. a) Schematic representation of a single unit and a layer of aminoclay (AC), which was covalently functionalized with aminopropyl groups. b) AC with aminopropyl groups on their surface formed hydrogels, and the hydrogels then are used to absorb different anionic dyes: coronene tetracarboxylate salt (blue) and perylene tetracarboxylate salt (green). Adapted from reference 139 with permission of The Royal Society of Chemistry.

4.2 Biomedical and pharmaceutical materials

4.2.1 Vehicles for drug delivery and controlled release

Polymeric hydrogels with an open network as drug vehicles normally undergo rapid drug release in an uncontrolled manner, causing drug distribution to various organs and compartments in body indiscriminately.[140] Hydrogel structures with clay minerals have achieved the ability to tune drug release in addition to improving resistance of loaded drugs from degradation .[141,142]The cationic drug species are bound to the CNPs via adsorption on the negatively charged clay mineral surface.[143] The binding of drugs onto montmorillonite results from a cation exchange reaction between cationic drug ions and cations in the interlayer space of clay minerals. In addition, a drug can also be attracted and loaded to CNPs by surface adsorption. By contrast, neutral drugs can simply be bound through their interactions with active sites on the surface of clay minerals in the network of hydrogels.[144]

Depending on drugs, CNPs and polymers, the interactions can be physical or chemical or both. The chemical adsorption is stronger than conventional physical adsorption. Importantly, in some nanocomposite hydrogel, clay minerals play a leading role in the adsorption of drugs.[145] For example, Anirudhan and Sandeep[146] studied the nanocomposite hydrogels consisting of carboxymethyl chitosan and montmorillonite and found that the negatively charged montmorillonite nanoplatelets encapsulated 94.56% of doxorubicin, a neutral drug, via hydrogen bonding and electrostatic interactions. The release of doxorubicin from the nanocomposite hydrogels was related to the breakage of the bonds and

hydrogel dissolution. Moreover, the addition of montmorillonite shifted the dissolution-resistant properties of hydrogels, thereby affecting the release of drugs.[147] Kevadiya et al.[148] synthesized montmorillonite/alginate nanocomposites hydrogels with the intercalation of lidocaine hydrochloride (LC), an antiarrhythmic local anesthetic drug, into montmorillonite. Due to the host-guest intercalation and the pH-responsiveness of the alginate/montmorillonite nanocomposites hydrogels, LC was released from montmorillonite in hydrogels in a controlled way. Kevadiya et al.[149] demonstrated that PAM/Na^+-montmorillonite nanocomposite hydrogels produced by free radical polymerization had the potential to be used as an anticancer drug carrier reservoir. The addition of the hydrophilic montmorillonite improved the water uptake of the nanocomposite hydrogels. *In vitro* study of drug release showed that the release from the nanocomposite hydrogels was controlled with time and partial diffusion through the swollen matrix of the nanocomposite hydrogel.[149] As shown by the above-mentioned examples, recent progress indicated that clay mineral-containing nanocomposite hydrogels have excellent potential as drug carriers.

4.2.2 Scaffold for tissue engineering

CNPs can combine with the macromolecules, such as poly(NIPAM-*co*-DMAEMA)),[150] PEO,[151] PVA, PAA, polypeptides,[152] alginate and chitosan[153] to form biocompatible nanocomposite hydrogels. Such hydrogels have been tested as scaffolds for organizing and directing cells to form a desired tissue and then the tissue is delivered in a minimally invasive manner.[154] Many kinds of cells, for example, the osteoblast,[72] murine fibroblast,[155] stem cells,[156] epithelial cells, human hepatic cells, dermal fibroblasts and umbilical vein endothelial cells[157] have showed good adhesion, differentiation and proliferation on the clay mineral-containing nanocomposite hydrogels *in vitro*.

The binding of the cell to the nanocomposite hydrogels surface is driven mainly by electrostatic interactions. For example, Kotobuki et al.[158] synthesized DMA nanocomposite hydrogels consisting of 2×10^{-2} mol/L of laponite for the cultivation, differentiation, and proliferation of human mesenchymal stem cell. Both the hydrophilic DMA and the charged laponite enhance the binding of cells to the nanocomposite hydrogels. Though PEG hydrogels are not an adhesive to cells, adding 5% of laponite as the cross-linker to form the PEG/laponite nanocomposite hydrogels enabled the materials to support cell adhesion.[102] The laponite in the covalently cross-linked network was mainly responsible for the

adhesion. Chang et al.[60] synthesized biocompatible PEGDA/laponite nanocomposite hydrogels that can support both two- and three-dimensional (2D and 3D) cell cultures. Unlike PEGDA hydrogels, PEGDA/laponite nanocomposite hydrogels supported cell adhesion and their subsequent spreading in a 2D culture and supported 3D cell encapsulation similar to that of widely used PEGDA hydrogel systems. Moreover, the addition of laponite wielded no adverse effect on the encapsulated cells. Similarly, adding 20–70% of laponite NPs to PEO, Gaharwar et al.[159] prepared nanocomposite hydrogels with higher cell viability (~95%) than that on a PEO hydrogel. The presence of montmorillonite also enhanced the cellular uptake efficiency of carboxymethyl chitosan nanocomposite hydrogels through hydrogen bonding. The nanocomposite hydrogels maintained good cell viability even after 96 h.[146] Due to the addition of laponite XLG to poly(2-methoxyethyl acrylate) (PMEA)-based hydrogels, the cells were successfully cultured on the surfaces of nanocomposite hydrogels.[160] The adhesion and proliferation of cells increased with the increasing concentration of laponite in the range of 10-23 wt%. Clearly, the CNPs-containing nanocomposite hydrogels have enhanced mechanical properties and hence possesses potential to be used as scaffolds for tissue engineering. Additionally, the ability of the nanocomposite hydrogels to support 3D culture of encapsulated cells establishes them as an ideal injectable system with minimally invasive strategies for *in vivo* applications.

4.2.3 Biosensor

Clay mineral-based materials have long been considered as biosensors.[161] Combined with stimuli-responsiveness to environment of the polymeric hydrogels, clay mineral-containing nanocomposite hydrogels as biosensors have additional advantages. Namely, the clay mineral-containing nanocomposite hydrogels consist of two basic components: (1) a recognition system and (2) a specific place for the sensitivity to occur. Earlier, by coating a silicon-integrated thermotransducer with a thin PAM/montmorillonite hydrogel membrane, which have time-dependent water vapor absorption, Gao et al.[162] successfully made a sensor with high selectivity and high sorption capacity for liquid water and water vapor. Such sensor showed an excellent reproducibility of the signal output voltage. A recent breakthrough by Ikeda et al.[163] featured a semi-wet fluorescent sensor by integrating supramolecular hydrogels with montmorillonite. Meanwhile, cationic coumarin dyes

were intercalated into the interlayer space of montmorillonite for probing spermine and spermidine, which can be used as biomarkers for assessing the effectiveness of cancer chemotherapy (**Fig. 10**). In this system, the organic supramolecular fibers formed the hydrogel and acted as an immobilization matrix and the anionic montmorillonite NPs played a critical role in the interactions between fluorescent molecules and biomarkers. Namely, the montmorillonite NPs served as host for aggregation of the exchangeable cationic fluorescent dyes and then such exchangeable cations that can be replaced by polyamines through electrostatic interactions and detected upon the color changes. As a result, color changes can be detected even with naked eyes in a user-friendly manner. Such a novel methodology provides a promising way to early cancer diagnosis in urine. This functional clay mineral-containing supramolecular hydrogel can also be taken as a model for designing sensor systems for a variety of analytes. In addition to montmorillonite, laponite was also used as a host to provide space for transforming signals in the hydrogel biosensor.[164] Importantly, both the polymer and clay minerals can be further modified with functional groups to optimize sensitivity and selectivity for targeted biomolecules.

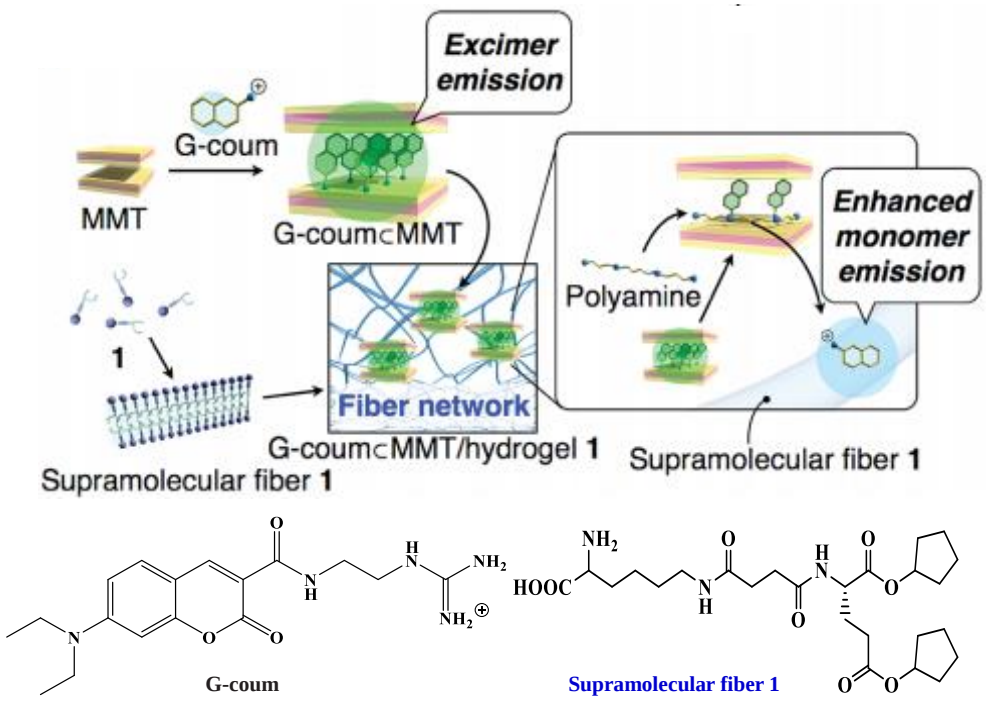

Fig. 10. Hybrid biosensor consists of a cationic fluorescent coumarin dye (G-coum) intercalated into supramolecular fiber 1/montmorillonite (MMT) hydrogels for determination of polyamines. The adsorbed cationic dyes in the interlayer space showed a weak greenish, which converted to an intensified blue color. Adapted and reprinted with permission from reference 163. Copyright (2011) American Chemical Society.

4.2.4 Wound dressing

Wound dressings are often used to accelerate the wound healing and create a moist environment. Meanwhile, an ideal wound dressing should be able to absorb the wound exudates and protect the wound from secondary infections.[165] The addition of clay minerals to the polymeric hydrogels and the interactions with polymers can improve the mechanical properties and absorptivity of nanocomposite hydrogels.[166] The clay mineral-containing nanocomposite hydrogel with suitable strength and elasticity is expected to be an effective wound dressing material. Moreover, due to the enhancement of adsorption caused by CNPs, the nanocomposite hydrogels can better absorb the wound exudates and keep the wound clean.[84] In addition, the clay mineral-containing nanocomposite hydrogels with a large amount of water can keep the wound moist, and protect the wound from infection.

Furthermore, CNPs in the hydrogels can tune the viscosity. Shen et al.[167] prepared the PAA/laponite nanocomposite hydrogels showing adjustable viscosity by adjusting the amount of laponite. The increased viscosity is beneficial for the wound dressing to adhere into wound tightly. Particularly, when the organically modified CNPs are used, it is possible for the hydrophobic organo-CNPs to encapsulate organic drugs and control the release of the drugs. Using the freezing–thawing method, Kokabi et al.[84] prepared PVA/CTA^+-montmorillonite nanocomposite hydrogels (CTA^+: cetyl trimethyl ammonium cation) as wound dressings. The addition of CTA^+-montmorillonite plays a key role for nanocomposite hydrogels to obtain relatively high adsorption capacity, appreciable vapor transmission rate, excellent barrier against microbe penetration, and excellent mechanical properties. The amount of the clay added to the nanocomposite hydrogel was found to be a key factor in such properties required for wound dressing.

In vivo evaluation on such PVA/organoclay nanocomposite hydrogel as an applicable wound dressing on animals also showed an improved healing process for wounds.[85] The improvement was attributable to better creation of moist surfaces on the wound with less scar formation, shorter duration of healing operation and better closing of the wound edges with enhanced tensile properties of the healed wound, i.e., tensile strength and elongation at break. Additionally, an *in vitro* cytotoxic assay showed that the as-prepared nanocomposite hydrogel was non-toxic and biocompatible. Particularly, when the organically modified CNPs are used, it is possible for the hydrophobic organo-CNPs to

encapsulate organic drugs, and control the release of the drugs. Importantly, in this way, organic drugs, which inherently cannot dissolve in water, can be introduced into the hydrogel using the organo-CNPs as the intermediary. Yet this strategy is rarely reported at present for clay mineral-containing nanocomposite hydrogels.

5. Conclusions and outlook

Exfoliated clay minerals with a high aspect ratio are unique functional colloidal 2D nanoplatelets, which can be incorporated into hydrophilic polymers to form a novel class of nanocomposite hydrogels. The inorganic clay nanoplatelets physically and/or chemically interact with a polymer matrix, thereby causing a dramatic improvement in mechanical properties, swellability, and adsorption of the resultant hydrogels. The stimuli-responsiveness of the nanocomposite hydrogels to temperature, pH and even electric field can also be significantly tuned by adding clay minerals into the hydrogels. The clay mineral-containing hydrogels may hence serve as model systems to investigate mechanisms of preparation and performance for many other two-dimensional inorganic nanosheets.

Substantial advances in such nanocomposite hydrogels have been achieved over the past few years. Nevertheless, to manufacture clay mineral-containing nanocomposite hydrogels in an effective way, and to endow the hydrogels with superior properties still faces challenges.

(1) Due to the additional interfacial interactions in the nanocomposite hydrogels, the analysis of particular interactions and the mechanisms of the performance enhancements become more complicated and the fundamental reasons remain elusive. Thus, further work is required to investigate the interactions that are intrinsic to these unique properties. Such mechanistic understanding will provide in-depth insights into the structure-function relationships, which is critical for formulating controlled preparations for desired applications. As such, there is a need for precise microstructural determination of interfacial and colloidal phenomena, *in-situ* observation of the hydrogel-forming, and linking at the molecular and atomic levels. To this end, computer simulation and theoretical calculations may also assist theoretical modeling, prediction, and description of the structure and properties of clay mineral-containing nanocomposite hydrogels.

(2) The *in situ* free radical polymerization is a common method to prepare nanocomposite hydrogels,

because of adaptability to various clay minerals and monomers. Currently, the rapid supramolecular assembly and the freezing-thawing process method are merely applicable to a few macromolecules or polymers. For these two methods, there is a large research space for rationally designing macromolecules or polymers with functional groups so that the resultant hydrogel meets the need for greater biocompatibility, faster response to stimuli, and increased mechanical properties. In addition, efficient exfoliation methods for clay minerals will require further development as uniformly-distributed CNPs in nanocomposite hydrogels are a key indicator of effectiveness for all preparation methods, and for performance of the nanocomposite hydrogels.

(3) The applications of clay mineral-containing nanocomposite hydrogels cover a spectrum spanning from superabsorbents for wastewater treatment to biomaterials. In particular, the clay mineral-containing nanocomposite hydrogels are attractive as vehicles for controlled encapsulation and release of drugs, as tough and adjustable scaffolds for tissue engineering, as nano-sized biosensors for diagnosis, and as wet and soft dressings for wound-healing. Nevertheless, most studies are still conducted at a laboratory scale. The biological stability and the side effects of nanocomposite hydrogels require *in vivo* investigations. In addition, there are rarely studies on the use of the clay mineral-containing nanocomposite hydrogels in notch-sensitivity and self-healing ability, and as cell-emulating system for photocatalysis.[80] Finally, more attention is required in combining the advantages of layered clay minerals and polymers, both of which can be modified and functionalized diversely. As such, many new possibilities will manifest for developing clay-containing hydrogel soft materials with unusual functions and wide applications.

Abbreviations

Polymers:

LLDPE: linear low density polyethylene
PAA: poly(acrylic acid)
PAM: polyacrylamide
PAMPSA: poly(2-acrylamido-2-methylpropane sulfonic acid)
PDMA: poly(*N*,*N*-dimethylacrylamide)
PEG: poly(ethylene glycol)
PEGDA: poly(ethylene glycol) diacrylate
PEGDMA: poly(ethylene glycol) dimethacrylate
PEO: polyethylene oxide
PMEA: poly(2-methoxyethyl acrylate)

PNIPAM: poly(*N*-isopropyl acrylamide)
POP: polyoxypropylene
PVA: poly(vinyl alcohol)
PVP: poly(*N*-vinyl-2-pyrrolidone)

Monomers for copolymerization:

AAG: acrylamide glycolic acid
DMAEMA: 2-(dimethylamino) ethyl methacrylate
DMAPMA: *N*-[3-(dimethylamino)propyl] methacrylamide
SMA: sodium methacrylate
SSNa: sodium 4-styrene sulfonate

Others:

AMO: amine-terminating Mannich oligomers
APS: ammonium persulfate
APTMA: (3-acrylamidopropyl) trimethylammonium
BP: benzoyl peroxide
CNPs: clay mineral nanoplatelets
CTAB: cetyltrimethyl ammonium bromide
CV: crystal violet
KPS: potassium persulfate
LCST: lower critical solution temperature
LDH: layered double hydroxide
NMBA: *N,N*-methylene-(bis)-acrylamide
SGPT: sol-gel phase transition
TEMED: *N,N,N',N'*-tetramethylene diamine
TSPP: tetrasodium diphosphate decahydrate
VPT: volume phase transitions

Acknowledgments

The authors wish to acknowledge the financial support from the National Natural Scientific Foundation of China (21373185), the Distinguished Young Scholar Grants from the Natural Scientific Foundation of Zhejiang Province (ZJNSF, R4100436), ZJNSF (LQ12B03004), Zhejiang 151 Talents Project, and the projects (2010C14013 and 2009R50020-12) from Science and Technology Department of Zhejiang Provincial Government and the financial support by the open fund from Key Laboratory of Clay Minerals of the Ministry of Land and Resources, China, (2014-K02) and Engineering Research Center of non-metallic minerals of Zhejiang Province（ZD2015k07), Zhejiang Institute of Geology and Mineral Resource, China，and the State Key Laboratory Breeding Base of Green Chemistry-Synthesis Technology, Zhejiang University of Technology (GCTKF2014006). The authors also feel grateful to anonymous reviewers for their comments and suggestions which are much helpful for us to improve the manuscript.

References

1 K. Kabiri, H. Omidian, M. Zohuriaan-Mehr and S. Doroudiani, *Polym. Compos.*, 2011, **32**, 277-289.

2 J. Jagur-Grodzinzki, *Polym. Adv. Technol.*, 2010, **21**, 27–47.

3 T. Sun, T. Kurokawa, S. Kuroda, A. B. Ihsan, T. Akasaki, K. Sato, M. A. Haque, T. Nakajima and J. Gong, *Nat. Mater.*, 2013, **12**, 932–937.

4 J. Kopeček and J. Yang, *Polym. Int.*, 2007, **56**, 1078–1098.

5 L. A. Estroff and A.D.Hamilton, *Chem. Rev.*, 2004, **104**, 1201 – 1217.

6 E. A. Appel, M. W. Tibbitt, M. J. Webber, B. A. Mattix, O. Veiseh and R. Langer, *Nat. Commun.*, 2015, **6**,

6295.
7 L. Liu, X. Tang, Y. Wang, S. Guo, Int. J. Pharmaceut., 2011, 414, 6–15.
8 M. Moriyama, N. Mizoshita, T. Yokota, K. Kishimoto and T. Kato, *Adv. Mater.*, 2003, **15**, 1335-1338.
9 A. R. Hirst, B. Escuder, J. F. Miravet and D. K. Smith, *Angew. Chem. Int. Edn.*, 2008, **47**, 8002–8018.
10 M. K. Shin, G. M. Spinks, S. R. Shin, S. I. Kim and S. J. Kim, *Adv. Mater.*, 2009, **21**, 1712-1715.
11 X. Liu, T. Zhou, Z. Du, Z. Wei and J. Zhang, *Soft Matter*, 2011, **7**, 1986-1993.
12 L. Xia, R. Xie, X. Ju, W. Wang, Q. Chen and L. Chu, Nat. Commun., 2013, **4**, 2226-2236.
13 K. Adesanya, E. Vanderleyden, A. Embrechts, P. Glazer, E. Mendes and P. Dubruel, *Appl. Polym. Sci.*, 2014, **131**, 41195-41203.
14 S. Varghese, A. K. Lele, D. Srinivas, M. Sastry and R. A. Mashelka, *Adv. Mater.*, 2001, **13**, 1544-1548.
15 D. G. Barrett, D. E. Fullenkamp, L. He, N. Holten-Andersen, K. Y. C. Lee and P. B. Messersmith, Adv. Funct. Mater., 2013, 23, 1111–1119.
16 P. D. Thornton, R. J. Mart and R. V. Ulijn, *Adv. Mater.*, 2007, **19**, 1252-1256.
17 T. S. Anirudhan and A. R. Tharun, *Chem. Eng. J.*, 2012, **181**, 761–769.
18 M. J. Zohuriaan-Mehr, H. Omidian, S. Doroudiani and K. Kabiri, *J. Mater. Sci.*, 2010, **45**, 5711-5735.
19 A. Musetti, K. Paderni, P. Fabbri, A. Pulvirenti, M. Al-Moghazy and P. Fava, *J. Food Sci.*, 2014, **79**, 577-582.
20 L. Dong, A. K. Agarwal, D. J. Beebe and H. R. Jiang, *Nature*, 2006, **442**, 551–554.
21 D. J. Beebe, J. S. Moore, J. M. Bauer, Q. Yu, R. H. Liu, C. Devadoss, B. H. Jo, *Nature*, 2000, **404**, 588-590.
22 G. Cirillo, F. P. Nicoletta, M. Curcio, U. G. Spizzirri, N. Picci and F. Iemma, *React. Funct. Polym.*, 2014, **83**, 62-69.
23 N. Sahiner and F. Seven, *Energy*, 2014, **71**, 170-179.
24 M. A. Alam, M. Takafuji and H. Ihara, *Polym. J.*, 2015, **46**, 293–300.
25 A. K. Gaharwar, N. A. Peppas and A. Khademhosseini, *Biotechnol. Bioeng.*, 2014, **111**, 441-453.
26 N. S. Satarkar, D. Biswal and J. Z. Hilt, *Soft Matter*, 2010, **6**, 2364–2371.
27 C. Zhou and J. Keeling, *Appl. Clay Sci.*, 2013, **74**, 3–9.
28 D. Zhang, C. Zhou, C. Lin, D. Tong and W. Yu, *Appl. Clay Sci.*, 2010, **50**, 1–11.
29 N. Iyi, Y. Ebina and T. Sasaki, *Langmuir*, 2008, **24,** 5591-5598.
30 J. N. Coleman, M. Lotya, A. O'Neill, S. D. Bergin, P. J. King and U. Khan, *Science*, 2011, **331**, 568-571.
31 V. Nicolosi, C. Manish, M. G. Kanatzidis, M. S. Strano and J. N. Coleman, *Science*, 2013, **340**, 1420-1438.
32 K. Haraguchi and T. Takehisa, *Adv Mater.*, 2002, **14**, 1120–1124.
33 T. Huang, *Appl. Phys. A*, 2012, **107**, 905–909.
34 K. Haraguchi and H. J. Li, *Macromolecules*, 2006**, 39**, 1898–1905.
35 J. Wang, L. Lin, Q. Cheng and L. Jiang, *Angew. Chem. Int. Ed.*, 2012, **51**, 4676–4680.
36 J. Ma, Y. Xu, Q. Zhang, L. Zha and B. Liang, *Colloid Polym Sci.*, 2007, **285**, 479–484.
37 A. B. Imran, T. Seki and Y. Takeoka, *Polym. J.*, 2010, **42**, 839–851.
38 W. F. Lee and L. L. Jou, *J. Appl. Polym. Sci.*, 2004, **94**, 74–82.
39 N. Y. Kostina, S. Sharifi, A. de los Santos Pereira, J. Michálek, D. W. Grijpmabc and C. Rodriguez-Emmenegger, *J. Mater. Chem. B*, 2013, **1**, 5644–5650.
40 S. Miyazaki, H. Endo, T. Karino, K. Haraguchi and M. Shibayama, *Macromolecules*, 2007, **40**, 4287-4295.
41 K. Haraguchi and D. Varade, *Polymer*, 2014, **55**, 2496–2500.
42 F. H. A. Rodrigues, A. G. B. Pereira, A. R. Fajardo and E. C. Muniz, *J. Appl. Polym. Sci.*, 2013, **128**, 3480–3489.
43 D. A. Young and D. E. Smith, *J. Phys. Chem. B*, 2000, **104**, 9163-9170.
44 C. C. Wang, L. C. Juang, C. K. Lee, T. C. Hsu, J. F. Lee and H. P. Chao, *J. Colloid Interf. Sci.*, 2004, **280**, 27–35.
45 J. Zhao, A. B. Morgan and J. D. Harris, *Polymer*, 2005, **46**, 8641–8660.
46 T. R. Guimarães, T. de C. Chaparro, F. D'Agosto, M. Lansalot, A. M. D. Santos and E. Bourgeat-Lami, *Polym. Chem.*, 2014, **5**, 6611-6622.
47 C. C. Chu, M. L. Chiang, C. M. Tsai and J. J. Lin, *Macromolecules*, 2005, **38,** 6240-6243.
48 P. Mongondry, T. Nicolai and J. F. Tassin, *J. Colloid Interf. Sci.*, 2004, **275**, 191–196.
49 P. Chen, S. Xu, R. Wu, J. Wang, R. Gu and J. Du, *Appl. Clay Sci.*, 2013, **72**, 196-200.
50 Y. C. Wang, T. K. Huang, S. H. Tung, T. M. Wu and J. J. Lin, *Sci. Rep.*, 2013, **3**, 2621.
51 L. Xiong, X. Hu, X. Liu and Z. Tong, *Polymer*, 2008, **49**, 5064–5071.
52 K. Haraguchi, *Polym. J.*, 2011, **43**, 223–241.
53 P. Li, N. H. Kim, D. Hui, K. Y. Rhee and J. H. Lee, *Appl. Clay Sci.*, 2009, **46**, 414–417.
54 X. Hu, L. Xiong, T. Wang, Z. Lin, X. Liu and Z. Tong, *Polymer*, 2009, **50**, 1933–1938.
55 M. Fukasawa, T. Sakai, U. Chung and K. Haraguchi, *Macromolecules*, 2010, **43**, 4370–4378.
56 H. Takeno and W. Nakamura, *Colloid Polym Sci.*, 2013, **291**, 1393-1399.
57 M. J. A. Oliveira, E. O. Silva, L. M. A. Braz, R. Maia, V. S. Amato, A. B. Lugão and D. F. Parra, *Radiat. Phys. Chem.*, 2014, **94**, 194–198.
58 Q. Wang, J. L. Maynar, M. Yoshida, E. Lee, M. Lee, K. Okuro, K. Kinbara and T. Aida, *Nature*, 2010, **463**, 339-343.
59 M. Sirousazar, M. Kokabi and Z. M. Hassan, *J. Biomat. Sci. Polym. E.*, 2011, **22**, 1023-1033.
60 C. W. Chang, A. van Spreeuwel, C. Zhang and S. Varghese, *Soft Matter*, 2010, **6**, 5157–5164.

61 A. K. Gaharwar, V. Kishore, C. Rivera, W. Bullock, C. J. Wu, O. Akkus and G. Schmidt, *Macromol. Biosci.*, 2012, **12**, 779–793.
62 E. Loizou, P. Butler, L. Porcar and G. Schmidt, *Macromolecules*, 2006, **39**, 1614–1619.
63 A. Nelson and T. Cosgrove, *Langmuir*, 2004, **20**, 2298–2304.
64 K. Haraguchi and H. J. Li, *J. Polym. Sci. Polym. Phys.*, 2009, **47**, 2328–2340.
65 O. Okay and W. Oppermann, *Macromolecules*, 2007, **40**, 3378–3387.
66 M. Shen, L. Li, Y. Sun, J. Xu, X. Guo, and R. K. Prud' home, *Langmuir*, 2014, **30**, 1636-1642.
67 M. Irani, H. Ismail and Z. Ahmad, *Polym. Test.*, 2013, **32**, 502-512.
68 P. Li, Siddaramaiah, N. H. Kim, S. B. Heo and J. H. Lee, *Composites: Part B*, 2008, **39**, 756–763.
69 K. Haraguchi, T. Takehisa and S. Fan, *Macromolecules*, 2002, 35, 10162–10171.
70 B. Urbano and B. L. Rivas, *Polym. Bull*, 2011, **67**, 1823–1836.
71 Y. Wang, W. Wang and A. Wang, *Chem. Eng. J.*, 2013, **228**, 132–139.
72 K. Kabiri, H. Mirzadeh, M. J. Zohuriaan-Mehra and M. Daliric, *Polym. Int.*, 2009, **58**, 1252–1259.
73 K. Kabiri, H. Mirzadeh and M. J. Zohuriaan-Mehra, *J. Appl. Polym. Sci.*, 2010, **116**, 2548–2556.
74 S. G. Starodoubtsev, A. A. Ryabova, A. R. Khokhlov, G. Allegra, A. Famulari and S. V. Meille, *Langmuir*, 2003, **19**, 10739–10746.
75 M. Liu, W. Li, J. Rong and C. Zhou, *Colloid Polym. Sci.*, 2012, **290**, 895–905.
76 Y. Yagci, S. Jockusch, and N. J.Turro, *Macromolecules*, 2010, **43**, 6245-6260.
77 H. Kazutoshi and T. Tetsuo, *Macromolecules*, 2010, **43**, 4294–4299.
78 C. Altinkok, T. Uyar, M. A. Tasdelen and Y. Yagci, *J. Polym. Sci. Pol. Chem.*, 2011, **49**, 3658-3663.
79 S. Tamesue, M. Ohtani, K. Yamada, Y. Ishida, M. Spruell, N. A. Lynd, C. J. Hawker and T. Aida, *J. Am. Chem. Soc.*, 2013, **135**, 15650−15655.
80 A. S. Weingarten, R. V. Kazantsev, L. C. Palmer, M. McClendon, A. R. Koltonow, A. P. S. Samuel, D. J. Kiebala, M. R. Wasielewski and S. I. Stupp, *Nat. Chem.*, 2014, **6**, 964–970.
81 F. Song, L. Zhang, J. Shi and N. Li, *Colloid. Surface. B*, 2010, **81**, 486–491.
82 C. M. Hassan and N. A. Peppas, *Adv. Polym. Sci.*, 2000, **153**, 37-65.
83 M. Sirousazar, M. Kokabi and Z. M. Hassan, *J. Appl. Polym. Sci.*, 2012, **123**, 50–58.
84 M. Kokabi, M. Sirousazar and Z. M. Hassan, *Eur. Polym. J.*, 2007, **43**, 773–781.
85 S. M. Ibrahim and A. A. El-Naggar, *J. Thermoplast. Compos.*, 2012, **26**, 1332–1348.
86 N. Bitinis, M. Hernandez, R. Verdejo, J. M. Kenny and M. A. Lopez-Manchado, *Adv Mater.*, 2011, **23**, 5229–5236.
87 K. Haraguchi, *Macromol. Symp*, 2007, **256**, 120-130.
88 W. F. Lee and Y. T. Fu, *J. Appl. Polym. Sci.*, 2003, **89**, 3652-3660.
89 J. P. Maranchi, M. M. Trexler, Q. Guo and J. H. Elisseeff, *Int. Mater. Rev.*, 2014, **59**, 264-296.
90 A. Zadražil and F. Štěpánek, *Colloid. Surface. A*, 2010, **372**, 115–119.
91 N. Patil, J. Soni, N. Ghosh and P. De, *J. Phys. Chem. B*, 2012, **116**, 13913-13921.
92 M. Shibayama, T. Karino, S. Miyazaki, S. Okabe, T. Takehisa and K. Haraguchi, *Macromolecules*, 2005, **38**,10772-10781.
93 K. Haraguchi, *Curr. Opin. Solid St. M.*, 2007, **11**, 47-54.
94 P. Kujawa and F. M. Winnik, *Macromolecules*, 2001, **34**, 4130–4135.
95 K. Murata and K. Haraguchi, *J Mater Chem.*, 2007, **17**, 3385–3388.
96 Y. Liu, M. Zhu, X. Liu, W. Zhang, B. Sun, Y. Chen and H. J. P. Adlerb, *Polymer*, 2006, **47**, 1–5.
97 K. Haraguchi, R. Farnworth, A. Ohbayashi and T. Takehisa, *Macromolecules*, 2003, **36**, 5732–5741.
98 E. Helvacıoğlu, V. Aydın, T. Nugay, N. Nugay, B. G. Uluocak and S. Şen, *J. Polym. Res.*, 2011, **18**, 2341–2350.
99 M. Zhu, Y. Liu, B. Sun, W. Zhang, X. Liu, H. Yu, Y. Zhang, D. Kuckling and H. J. P. Adler, *Macromol. Rapid Commun.*, 2006, **27**, 1023–1028.
100 J. Nie, B. Du and W. Oppermann, *Macromolecules*, 2005, **38**, 5729-5736.
101 P. Schexnailder, E. Loizou, L. Porcar, P. Butler and G. Schmidt, *Phys. Chem. Chem. Phys.*, 2009, **11**, 2760-2766.
102 A. K. Gaharwar, C. P. Rivera, C. J. Wu and G. Schmidt, *Acta Biomater.*, 2011, **7**, 4139–4148.
103 M. Liu, Y. Ishida, Y. Ebina, T. Sasaki, T. Hikima, M. Takata and T. Aida, *Nature*, 2015, **517**, 68-72.
104 V. Can, S Abdurrahmanoglu and O. Okay, *Polymer*, 2007, **48**, 5016-5023.
105 H. Ren, M. Zhu and K. Haraguchi, *Macromolecules*, 2011, **44**, 8516–8526.
106 J. Zhang, L. Wang and A. Wang, *Ind. Eng. Chem. Res.*, 2007, **46**, 2497-2502.
107 Y. Xiang, Z. Peng and D. Chen, *Eur. Polym. J.*, 2006, **42**, 2125–2132.
108 J. Yi and L. Zhang, *Eur. Polym. J.*, 2007, **43**, 3215–3221.
109 Z. Darvishi, K. Kabiri, M. J. Zohuriaan-Mehr and A. Morsali, *J. Appl. Polym. Sci.*, 2011, **120**, 3453-3459.
110 H. Kaşgöz, A. Durmus and Ahmet Kaşgöz, *Polym Adv Technol*, 2008, **19**, 213-220.
111 J. Aalaie, E. Vasheghani-Farahani, A. Rahmatpour and M. A. Semsarzadeh, *Eur. Polym. J.*, 2008, **44**, 2024–2031.
112 W. Zhang, W. Luo and Y. Fang, *Mater. Lett.*, 2005, **59**, 2876-2880.

113 E. Al, G. Güçlü, T. B. İyim, S. Emik and S. Özgümüş, *J. Appl. Polym. Sci.*, 2008, **109**, 16–22.
114 X. Xia, J. Yih, N. A. D'Souza and Z. Hu, *Polymer*, 2003, **44**, 3389–3393.
115 A. Li, A. Wang and J. Chen, *Appl. Polym. Sci.*, 2004, **92**, 1596-1603.
116 J. Zhang and A. Wang, *React. Funct. Polym.*, 2007, **67**, 737–745.
117 S. K. Patra and S. K. Swain, *J. Appl. Polym. Sci.*, 2011, **120**, 1533-1538.
118 K. Haraguchi and H. J. Li, *Angew. Chem. Int. Ed.*, 2005, **44**, 6500–6504.
119 K. Haraguchi, *Colloid Polym Sci.*, 2011, **289**, 455–473.
120 C. Yao, Z. Liu, C. Yang, W. Wang, X. Ju, R. Xie and L. Chu, *Adv. Funct. Mater.*, 2015, **25**, 2980–2991.
121 R. A. Frimpong, S. Fraser and J. Z. Hilt, *J. Biomed. Mater. Res. A*, 2006, **10**, 1-6.
122 Q. Yang, N. Adrus, F. Tomicki and M. Ulbricht, *J. Mater. Chem.*, 2011, **21**, 2783-2811.
123 K. Haraguchi, K. Murata and T. Takehisa, *Macromolecules*, 2012, **45**, 385−391.
124 Y. Satokawa, T. Shikata, F. Tanaka, X. Qiu and F. M. Winnik, *Macromolecules*, 2009, **42**, 1400–1403.
125 L. W. Xia, R. Xie, X. J. Ju, W. Wang, Q. Chen, L. Y. Chu, *Nat. Commun.*, 2013, **4**, 2226-2236.
126 T. S. Anirudhan and S. Sandeep, *New J. Chem.*, 2011, **35**, 2869–2876.
127 Y. Li, D. Maciel, H. Tom as, Jo ão Rodrigues, H. Ma and X. Shi, *Soft Matter*, 2011, **7**, 6231–6238.
128 H. Li, R. Wu, J. Zhu, P. Guo, W. Ren, S. Xu and J. Wang, *J. Polym. Sci. Pol. Phys.*, 2015, **53**, 876–884**.**
129 M. Boruah, M. Mili, S. Sharma, B. Gogoi and S. K. Dolui, *polym. Composite.*, 2014, **36**, 34-41.
130 H. Zhang, J. Li, H. Cui, H. Li and F. Yang, *Chem. Eng. J.*, 2015, **259**, 814–819.
131 G. R. Mahdavinia, B. Massoumi, K. Jalili and G. Kiani, *J. Polym. Res.*, 2012, **19**, 9947-9959.
132 H. Kaşgöz, A. Durmus and A. Kaşgöz, *Polym. Adv. Technol.*, 2008, **19**, 213–220.
133 J. Yi and L. Zhang, *Bioresource Technol.*, 2008, **99**, 2182–2186.
134 A. S. Ozcan, B. Erdem and A. J. Ozcan, *J. Colloid. Interf. Sci.*, 2004, **280**, 44–54.
135 L. Wu, M. Ohtani, S. Tamesue, Y. Ishida and T. Aida, *J. Polym. Sci. Pol. Chem.*, 2014, **52**, 839-847.
136 G. Güçlü, E. Al, S. Emik, T. B. İyim, S. Özgümüş and M. Özyürek, *Polym. Bull.*, 2010, **65**, 333–346.
137 G. R. Mahdavinia, H. Aghaie, H. Sheykhloie, M. T. Vardini and H. Etemadi, *Polym.*, 2013, **98**, 358–365.
138 L. Zhang, Y. Zhou and Y. Wang, *J. Chem. Technol. Biotechnol.*, 2006, **81**, 799–804.
139 K. V. Rao, A. Jain and S. J. George, *J. Mater. Chem. C*, 2014, **2**, 3055-3064.
140 T. Vermonden, R. Censi and W. E. Hennink, *Chem. Rev.*, 2012, **112**, 2853−2888.
141 D. Depan, A. P. Kumar and R. P. Singh, *Acta Biomater.*, 2009, **5**, 93–100.
142 T. Takahashi, Y. Yamada, K. Kataoka and Y. J. Nagasaki, *J. Control. Release*, 2005, **107**, 408-416.
143 J. I. Dawson, J. M. Kanczler, X. B. Yang, G. S. Attard and R. O. C. Oreffo, *Adv. Mater.*, 2011, **23**, 3304–3308.
144 C. Wu and G. Schmidt, *Rapid Commun.*, 2009, **30**, 1492-1497.
145 C. Viseras, C. Aguzzi, P. Cerezo and M. C. Bedmar, *Mater. Sci. Techn-lond.*, 2008, **24**, 1020-1026.
146 T. S. Anirudhan and S. J. Sandeep, *Mater. Chem.*, 2012, **22**, 12888-12899.
147 M. Boruah, P. Gogoi, A. K. Manhar, M. Khannam, M. Mandal and S. K. Dolui, *RSC Adv.*, 2014, **4**, 3865–43873.
148 B. D. Kevadiya, G. V. Joshi, H. M. Mody and H. C. Bajaj, *Appl. Clay Sci.*, 2011, **52**, 364–367.
149 B. D. Kevadiya, R. R. Pawar, S. Rajkumar, R. Jog, Y. K. Baravalia, H. Jivrajani, N. Chotai, N. R. Sheth, H. C. Bajaj, *Biochemistry and Biophysics*, 2013, **1**, 43-60.
150 D. Liu, T. Wang, X. Liu and Z. Tong, *Biopolymers*, 2013, **101,** 58-65.
151 P. J. Schexnailder, A. K. Gaharwar, R. L. Bartlett, B. L. Seal and G. Schmidt, *Macromol. Biosci.*, 2010, **10**, 1416–1423.
152 G. Ozkoc, S. Kemaloglu and M. Quaedflieg, *Polym. Compos.*, 2010, **31**, 674–683.
153 H. Zhuang, J. Zheng, H. Gao and K. De Yao, *J. Mater. Sci.: Mater. Med.*, 2007, **18**, 951–957.
154 J. L. Drury and D. J. Mooney, *Biomaterials*, 2003, **24**, 4337–4351.
155 Q. Jin, P. Schexnailder, A. K. Gaharwar and G. Schmidt, *Macromol. Biosci.*, 2009, **9**, 1028-1035.
156 H. L. Lim, J. C. Chuang, T. Tran, A. Aung, G. Arya and S. Varghese, *Adv. Funct. Mater.*, 2011, **21**, 55-63.
157 K. Haraguchi, T. Takehisa and M. Ebato, *Biomacromolecules*, 2006, **7**, 3267-3275.
158 N. Kotobuki, K. Murata and K. Haraguchi, *J. Biomed. Mater. Res. Part A*, 2013, **101**, 537–546.
159 A. K. Gaharwar, P. Schexnailder, V. Kaul, O. Akkus, D. Zakharov, S. Seifert and G. Schmidt, *Advan. Funct. Mater.*, 2010, **20**, 429-436.
160 K. Haraguchi, S. Masatoshi, N. Kotobuki and K. Murata, *J. Biomater. Sci. Polym. Ed.*, 2011, **22**, 2389–2406.
161 N. An, C. Zhou, X. Zhuang, D. Tong and W. Yu, *Appl. Clay Sci.*, 2015, **114**, 283-296.
162 D. Gao, R. B. Heimann, J. Lerchner, J. Seidel and G. Wolf, *J. Mater. Sci.*, 2001, **36**, 4567-4571.
163 M. Ikeda, T. Yoshii, T. Matsui, T. Tanida, H. Komatsu and I. Hamachi, *J. Am. Chem. Soc.*, 2011, **133**, 1670–1673.
164 Q. Shi, Q. Li, D. Shan, Q. Fan and H. Xue, *Mat. Sci. Eng. C-Mater.*, 2008, **28**, 1372-1375.
165 S. Y. Lin, K. S. Chen and L. Run-Chu, *Biomaterials*, 2001, **22**, 2999–3004.
166 T. S. Anirudhan, S. S. Gopal and S. Sandeep, *Appl. Clay Sci.*, 2014, **88-89**, 151–158.
167 M. Shen, L. Li, Y. Sun, J. Xu, X. Guo and R. K. Prud'homme, *Langmuir*, 2014, **30**, 1636−1642.

RE: Soft Matter - SM-REV-05-2015-001277.R2

A table of contents entry

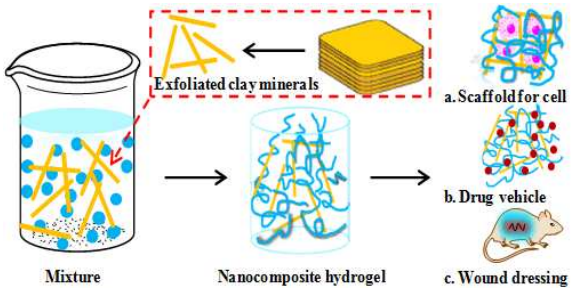

Clay-containing nanocomposite hydrogels, made from polymerization, supramolecular assembly or freezing–thawing cycles, are exceptional in formation mechanisms, properties and applications.